IEEE Access
Multidisciplinary | Rapid Review | Open Access Journal

Received October 9, 2018, accepted October 26, 2018, date of publication November 9, 2018, date of current version December 3, 2018.

Digital Object Identifier 10.1109/ACCESS.2018.2879902

Wireless Channel Models for Maritime Communications

JUE WANG[1,2], (Member, IEEE), HAIFENG ZHOU[1], YE LI[1,2], (Member, IEEE), QIANG SUN[1,2], YONGPENG WU[3], (Senior Member, IEEE), SHI JIN[4], (Member, IEEE), TONY Q. S. QUEK[5], (Fellow, IEEE), AND CHEN XU[1]

[1]School of Electronic and Information Engineering, Nantong University, Nantong 226019, China
[2]Nantong Research Institute for Advanced Communication Technologies, Nantong 226019, China
[3]Department of Electrical Engineering, Shanghai Jiao Tong University, Shanghai 200240, China
[4]National Communications Research Laboratory, Southeast University, Nanjing 210096, China
[5]Information Systems Technology and Design Pillar, Singapore University of Technology and Design, Singapore 487372

Corresponding author: Qiang Sun (sunqiang@ntu.edu.cn)

This work was supported in part by the National Natural Science Foundation of China under Grant 61771264, Grant 61801248, and Grant 61501264, in part by the Nantong University-Nantong Joint Research Center for Intelligent Information Technology under Grant KFKT2016B01, Grant KFKT2017B01, and Grant KFKT2017A04, and in part by the Natural Science Foundation of the Higher Education Institutions of Jiangsu Province, China under Grant 18KJB510036. The work of Y. Wu was supported in part by the National Science Foundation (NSFC) under Grant 61701301 and in part by the Young Elite Scientist Sponsorship Program by CAST. The work of S. Jin was supported by the National Science Foundation (NSFC) for Distinguished Young Scholars of China under Grant 61625106.

ABSTRACT Recently, broadband maritime communication has attracted much attention due to the rapid development of blue economy. In addition to the conventional MF/HF/VHF bands, there has been increasing interests in the utilization of higher frequency bands to provide broadband data service to the sea area. To design efficient maritime communication systems, the first and a fundamental requirement is to develop a framework to understand the wireless channels. In an integrated air-ground-sea communications network, there are two major type of channels to be investigated, namely the air-to-sea channel (e.g., for communication links from the aircraft-based base stations or relays) and the near-sea-surface channel (for land-to-ship/ship-to-land or ship-to-ship communications). Due to the unique features of the maritime propagation environment such as sparse scattering, sea wave movement, and the ducting effect over the sea surface, the modeling of these maritime channel links differs from conventional terrestrial wireless channels in many aspects and, consequently, will result in significant impact on the transceiver design. In this survey, we highlight the most notable differences from the modeling perspective as well as the channel characteristics for the air-to-sea and near-sea-surface channel links, with more focus on the latter. After a thorough review of existing modeling approaches and measurement campaigns, we conclude that the *sparse* and the *location-dependent* properties constitute the most important and distinctive characteristics of the maritime wireless channels. As such, we further remark on the challenges and research topics for future development of maritime communications.

INDEX TERMS Maritime communications, channel model, evaporation duct, finite scattering, beyond line-of-sight.

I. INTRODUCTION

In the past decades, the world has witnessed the ever-growing of maritime economy. Conventional industries such as fishery and transportation have been continuously developed, while new maritime activities including oil exploitation, environment monitoring and tourism have emerged. All these require higher data rate and more reliable wireless communications. Existing maritime communication systems mainly rely on satellite and/or customized communication systems operating in MF/HF/VHF bands, such as the navigational telex (NAVTEX) system, the automatic identification system (AIS), and the developing VHF data exchange system (VDES) [1], [2]. Therefore, the conventional maritime networks are usually viewed as integrated satellite-ground-sea networks with mesh topology among the users [3]–[6]. The satellite-based solution, albeit undergoing

fast development which greatly enhances its ability of providing high-speed data coverage for a wide area, suffers from inevitable large propagation delay and high implementation cost. On the other hand, the MF/HF/VHF-based systems, usually being adopted for vessel identification, tracking/monitoring and security alerting, also have inherent problems such as the requirement of special devices and insufficient bandwidth.

To improve user experience, it is desirable for a near coast maritime user to be able to access seamlessly high-speed terrestrial mobile networks (like 4G or 5G networks) in the near future.[1] As a result, near coast maritime communications have drawn considerable attention, where the main objective is to provide wide-area broadband coverage for offshore users with the aid of terrestrial base stations (BSs) and/or relays, and with the technologies adopted for WiFi [7], [8], WiMAX [9]–[13] and LTE [14]–[16]. For example, the TRI-media Telematic Oceanographic Network (TRITON) [17], the Nautical Ad-Hoc Network (NANET) [18], and the MarCom project [19] have been designed to provide high-speed data coverage to offshore areas and reliable inter-ship communication links. To extend the coverage, the BLUECOM+ project has been conducted to cover a vast sea area with the aid of balloon-based relays [20], [21]. Similarly, some other works have considered to use unmanned aerial vehicle (UAV) in maritime communications [22]. Furthermore, 5G techniques such as massive multiple-input multiple-output (MIMO), millimeter wave (mmWave), and user-centric network, can potentially provide a higher data rate coverage to widely distributed maritime users [23]–[25]. The application of these physical layer techniques and network architectures is foreseen to be a promising direction in future maritime communication systems.

To design an efficient maritime communication system, it is fundamental to understand the corresponding wireless channels well and develop appropriate channel models. Whereas the maritime satellite channel has been investigated extensively [26], the wireless channels in the integrated air-ground-sea network are less well understood for the near coast scenario. In both the academia and industry, researchers have recently launched several measurement campaigns and have proposed a number of modeling approaches to characterize the maritime wireless channels. The interested bands mainly focus on the unlicensed spectrum around 2.4 GHz [27], [28] and 5.2/5.8 GHz [29]–[34]. The 5G candidate mmWave frequency bands [35] have also attracted increasing interests given its potential to be integrated into the terrestrial networks.

In a near coast integrated air-ground-sea communication network, there are two major type of channel links to be considered, namely, the air-to-sea channel link which is used for the transmission from aircraft (balloons or UAVs)-based BSs or relays, and the near-sea-surface channel link which is used to support land-to-ship/ship-to-land and ship-to-ship communications. On the one hand, some air-to-ground wireless channel models have recently been modified to apply for the air-to-sea propagation environment [36]–[38]. On the other hand, the near-sea-surface channels have also been measured and discussed from different perspectives: The path loss models have been investigated in [32]–[34] and [39]–[43]; the geometry-based stochastic models (GBSM) under two-ray (see [11], [27], [35], [44], [45]) and three-ray (see [30], [46]) assumptions have been studied to describe the oscillation in the received signal strength, stemming from the sparse multipath propagation over the sea surface; the small-scale fading characteristics have been investigated in [27]–[29] and [47]–[50]; measurement and modeling for the near-sea-surface duct channel have been investigated in [51]–[63]. However, to the best of our knowledge, a comprehensive survey on the latest modeling approaches and measurement results for maritime wireless channels (especially for the new frequency bands) is still missing in the literature.

In this survey, we aim at providing a thorough review of the existing modeling approaches and measurement results for the maritime wireless channel, and highlight its key differences as compared to the channel models commonly adopted for terrestrial communications. We consider both the air-to-sea and near-sea-surface channels, while with more focus on the near-sea-surface channel link. From our review, we conclude that the two most important and distinctive features of the maritime wireless channels are *sparse* and *location dependant*: 1) The sparse feature is commonly seen in the maritime environment, in different aspects including both the scattering and the user distribution. 2) The location-dependant feature indicates that for a maritime user, totally different model structures should be applied for the channels in different location regions. Consequently to these features, new challenges and opportunities arise in the design of future maritime communication systems.

The remainder of this paper is organized as follows: In Section II, we first describe the propagation environment for maritime communications and highlight its key features. In Section III, the air-to-sea channel models are briefly reviewed and discussed. In Section IV, we focus on introducing the channel models used for the near-sea-surface communication links. Depending on the distance between the transmitter (Tx) and receiver (Rx), we present the large- and small-scale fading characteristics and the corresponding models for the LOS and beyond LOS (B-LOS) channels, respectively. In Section V, we conclude the key differences of maritime wireless channels. Finally, Section VI discusses future research topics and Section VII concludes this paper.

II. THE MARITIME RADIO PROPAGATION ENVIRONMENT

A typical near coast integrated air-ground-sea maritime communication network is illustrated in Fig. 1, where various communication links are adopted to guarantee

[1] In this paper, we use "near coast" for the region that is several tens (at most hundreds) kilometers away from the coast. In this region, wireless communication between land and a maritime user could be done without the aid of satellite.

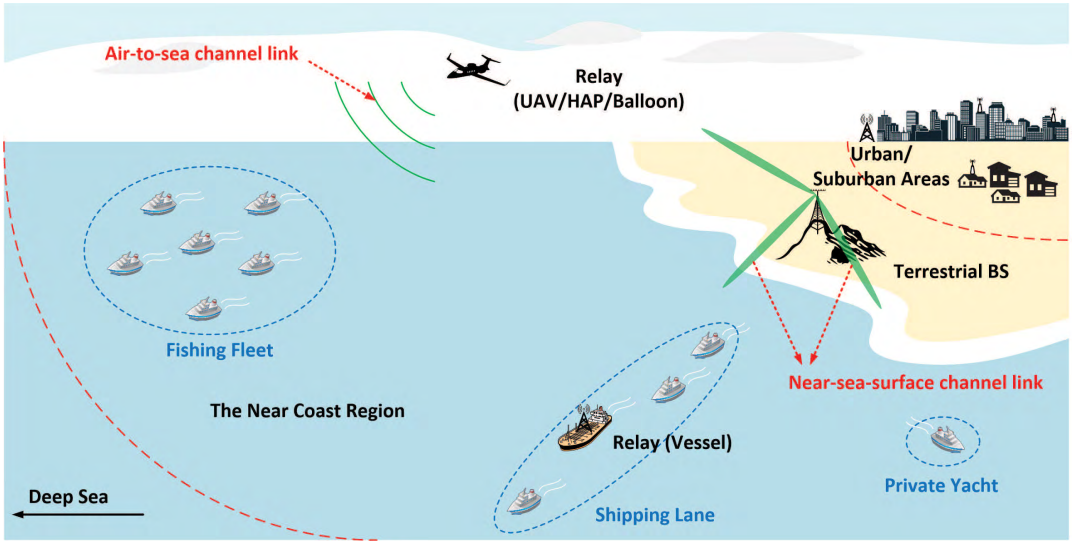

FIGURE 1. An illustration of the integrated air-ground-sea maritime communication network.

a wide coverage. In general, a near user can be directly served by the terrestrial BS. As the distance becomes larger, the use of relay nodes such as dedicated vessels or high altitude platforms (HAPs)/UAVs are needed. The maritime communication environment has several important features which will substantially affect the channel statistics and the channel modeling. In this section, we identify three such important features, namely sparsity, instability and the evaporation ducting phenomenon.

A. SPARSITY

Sparsity in the maritime channel modeling is mainly manifested in two aspects: sparse scattering and sparse user distribution.

First, the scattering of electromagnetic waves directly affects the multipath fading statistics of the channel. Due to the lacking of scatterers in the vast sea area, sparse scattering constitutes the most fundamental difference between the maritime wireless channels and the channels inland. The fact of sparse scattering holds for almost all the channel links shown in Fig. 1, including the air-to-sea, land-to-ship and ship-to-ship channels. For this reason, the Rayleigh fading, commonly assumed in the modeling and analysis of terrestrial communication systems in the rich scattering environment, is in general no longer suitable in most maritime environments. Instead, the finite scattering model structure such as that introduced in [64] and [65] could be more appropriate.

Due to sparsity, the following two paths are extremely important in the maritime channel modeling: 1) Since obstacles are scarcely presented in the sea, the LOS path will dominate most of the channel links in Fig. 1; 2) a reflection path from the sea surface may exist in some conditions. Considering these two paths, a two-ray channel model can be a good approximation when the antennas onboard are mounted high [11]. On the other hand, with relatively low onboard antenna height, local scatterers around the user will introduce more randomness in the wireless channel which cannot be ignored. For this case, more paths need to be taken into consideration, and the so-called two wave with diffusion power (TWDP) model, firstly introduced in [66] and recently generalized to the fluctuating two-ray (FTR) model [67], [68] in the analysis of mmWave communications, may provide a generic model structure.

Besides that in the number of multipath components (MPCs), sparsity also holds in the angle domain. For example, the LOS path and the sea-surface reflection path in the two-ray model may come from similar angular directions. The angle difference between these two paths decreases as the Tx-Rx distance increases. When multiple antenna arrays are deployed at the transmitter and/or receiver, this will lead to high correlation between the antenna elements, and subsequently a rank-deficient MIMO channel matrix.

Second, not only for the scattering, sparsity is also seen in the user distribution, because the maritime users are more likely to be widely distributed in a very vast sea area. This means that the large-scale fading of different users in the same network may be largely different, caused not only by the path loss effect, but also by other unpredictable reasons such as rain and air attenuations, which are not uniform over the vast sea area [69], [70]. These will then result in different large-scale fading distribution when modeling a maritime communications network as compared to that inland.

B. INSTABILITY

Unlike the users inland, the received signal strength at a maritime user may be fluctuant due to the so-called *link mismatch* caused by sea wave movement, even if the user is motionless at a fixed location. Such instability induced by waves would lead to periodic variations to the height and orientations of the onboard antennas. From the modeling perspective, the sea

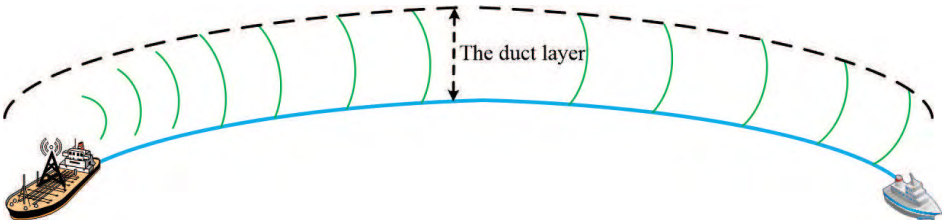

FIGURE 2. Illustration of the wave trapping effect in the evaporation duct layer (reproduced from [53, Fig. 1]).

wave is often described by a trochoid or sinusoidal motion, with the ship located at the tangent curve of the waves [71]. Accordingly, the influence on the onboard receivers can be divided into two parts, namely the linear motions and the rotational motions in the corresponding directions. These motions will subsequently cause variations in the received signal strength [72], [73]. It has been recorded that a variation of 1 m in the antenna height would result in a variation up to 13 dB in the received signal strength [74]. This suggests that for maritime communications, predicting the path loss simply based on the user's location may lead to inaccurate results. Taking into account the randomness caused by sea waves in the modeling is necessary.

Besides the link mismatch effect, the sea wave movement will also affect the scattering in the radio propagation, especially for the surface reflection paths. Three parameters, namely the *significant sea wave height*, the *average sea wave length*, and the *average sea wave period* are usually used to describe the sea wave movement [75], [76]. In the Pierson-Moskowitz sea state table, the sea state is classified into 10 levels from calm to rough according to the values of these parameters [77]. With fierce sea wave movement (i.e., high sea state levels), the incoming wavefronts encounter more scattering and/or reflections due to the rough sea conditions. In this case, the simplified two-ray model has to be modified with the help of the so-called Karasawa's model [78], which accounts for: 1) the variation of the sea surface height when calculating the amplitude of the main reflection path, and 2) multiple scattered components stemming from irregular sea surface, which are characterized by dividing a large sea surface area into several small-sized regions and each corresponds to a individual scattering path. With these manipulations, the Karasawa's model is able to describe more precisely the multipath fading and path loss in the presence of rough sea conditions [31].

Overall, the sea wave movement substantially affects the stability of the maritime communication link. In [12], the IEEE 802.16j standard has been adopted for maritime e-Navigation communications. It was shown that the communication becomes infeasible at sea states 7 and 8, even with high transmit SNR. The impact of sea wave movement must be taken into consideration in the maritime channel modeling for the establishment of reliable and stable maritime communications.

C. EVAPORATION DUCTING PHENOMENON

The atmospheric ducting effect has been long noticed, and intensively investigated especially for radar systems and military communications. The ducting effect is caused by the refractivity changing at different heights of the atmosphere, which is caused by the change of atmospheric pressure, temperature and humidity etc. According to the differences in the appearance heights and formulation conditions, there exists three typical types of atmosphere ducts: the surface duct (including the evaporation duct), the surface-based duct, and the elevated duct. A comprehensive review of these ducts and their formulations is referred to [52] and [53].

Among all the atmospheric ducts, the evaporation duct (mainly caused by the water evaporation over the sea surface) is commonly utilized in maritime communications thanks to its ability of providing transhorizon transmission.[2] More importantly, the evaporation duct has appropriate appearance height (around 10m-20m, at most 40m) and high appearance probability (90% of the time in the equatorial and tropical areas) [53], [56], [57]. As illustrated in Fig. 2, the electromagnetic waves emitted in certain directions will be ''trapped'' between the sea surface and the evaporation duct layer. Thereby, the wireless energy can be concentrated in the intended direction instead of spreading over the entire free space, and hence enhances the coverage range [59]–[63].

The modeling of wireless propagation in the duct layer is critical for the design and analysis of B-LOS maritime communications. Related works were conducted mainly from two different perspectives: 1) Some works focused on the measurement and modeling of key physical parameters of the evaporation duct, including the refractivity and the duct height for different carrier frequencies, under different climate conditions [79], [80]; 2) other works aimed at describing the radio propagation in the evaporation duct layer as well as its properties such as the path loss [52], [55], [59], [62], using typical methods including the parabolic equation method and optical ray tracing method [53].

The three features described above will affect both the air-to-sea and near-sea-surface channel links in Fig. 1. In the following, we will describe the modeling of these two types of channel links considering these features,

[2]For the near coast region we concerned, transhorizon transmission needs to be considered when the height of the terrestrial BS is limited.

and highlight their key differences as compared to that inland.

III. AIR-TO-SEA CHANNELS

Whereas the air-to-ground channels have been intensively studied in the literature [81], [82], the three features of the maritime environment, i.e., sparsity, instability and ducting effect, bring unique characteristics to the air-to-sea channels and therefore result in notable differences in the channel modeling. Herein, we highlight some most distinctive properties of the air-to-sea radio propagation, as well as their impacts on the channel.

A. PHYSICAL PROPAGATION CHARACTERISTICS

In most cases, the LOS path and the surface reflection path are two dominant paths in an air-to-sea channel. Considering that the transmitter is in general at high altitude and the transmission distance is large, the so-called curved-Earth two-ray (CE2R) model is usually adopted to take into account the earth curvature [38]. In some scenarios, more scattered weak paths need to be considered besides the two dominant paths. The scattering generally happens around the receiver due to the high Tx altitude [82]. As mentioned, whereas the local scattering could be rich for inland receivers (e.g., in the near-urban area), a maritime user is expected to face much sparser scattering, and hence the over-water setting may simplify the modeling as compared to the inland air-to-ground channels. In [36], the channel over the water was described by a three-ray model, which consists of one LOS path and two reflection paths. The stronger reflection path stems from the direct reflection from the sea surface, and the weaker reflection path is formed by many electromagnetic waves from multiple weak sources of reflections.

In the three-ray model, the instability feature of the maritime propagation environment would affect the relative amplitudes of the two reflection paths. For calm sea surface, the stronger reflection path is expected to be more dominant. However, when the sea surface becomes ''rougher'' (i.e., when the sea state level is high), the strength of all reflection paths will be decreased, and the two reflection paths will become less distinguishable. In the extreme condition, the entire channel will be composed of one LOS path and only one reflection path. The single reflection path can be seen as superposition of multiple weak reflections. In case that the number of weak reflection paths is large, the three-ray model simply reduces to, statistically, the well known Rician fading for narrow band transmissions [38].

In the three-ray air-to-sea channel model, the existence of the third path also relies on parameters such as the carrier frequency, the Rx antenna height, and the number of maritime objects (e.g., vessels, reefs, offshore drilling platforms, etc.) [38]. Measurement results in [37] revealed that the maximum probability that the third path exists is 8.5% for the 5.7 GHz carrier frequency. With higher Rx antenna height, this probability may be even lower. Reference [37] has also observed that the third path usually has much lower strength than the other two paths, thereby the two-ray model can be a good approximation and provide a good fit to up to 86% of the measurement results. In this light, an air-to-sea tapped delay line channel model can be represented by

$$h_{3Ray}(t,\tau) = h_{2Ray}(t,\tau) + z_3(t)\, a_3(t) \exp\left(j\varphi_3(t)\right) \delta\left(\tau - \tau_3(t)\right), \quad (1)$$

where a_3, τ_3, and φ_3 are the time-varying amplitude, propagation delay, and phase shift of the third multipath component, respectively [38]. Here, z_3 is generated from a random process that controls the occurrence possibility of the third multipath component, and $h_{2Ray}(t,\tau)$ is the CE2R model with

$$h_{2Ray}(t,\tau) = \delta\left(\tau - \tau_0(t)\right) + \alpha_s(t) \exp\left(j\varphi_s(t)\right) \delta\left(\tau - \tau_s(t)\right), \quad (2)$$

where $\alpha_s(t)$ is the amplitude of the surface reflection wave, and $\varphi_s(t)$ is the relative phase shift to the direct path. $\alpha_s(t)$ might be affected by parameters including the reflection coefficient, shadowing factor, divergence factor and the surface roughness factor, and $\varphi_s(t)$ can be geometrically calculated according to the curved earth approximation (See [38, Fig. 21]).

B. KEY PARAMETERS OF THE AIR-TO-SEA CHANNEL

In this subsection, we highlight some measurement results for various key parameters of the air-to-sea channels, including the path loss, the root mean square-delay spread (RMS-DS) and the Rician K-factor. The readers are referred to [38] for a more detailed description of the latest results.

1) PATH LOSS

As discussed, the air-to-sea channel can be approximated by a classic two-ray or three-ray model. In this case, due to the destructive summation of the two or three independent rays with different phases, the channel will meet deep nulls at certain Rx positions as confirmed by [37] and [38].[3] The deep nulls appear with higher probability in the maritime environment due to its sparse nature, while for the inland air-to-ground channels, the path loss curve would be smoother with rich scattering.

Two factors that may affect the path loss model need to be considered in the air-to-sea propagation environment: 1) *Earth curvature:* In maritime communications, usually long coverage distance is expected. Therefore, the application of the CE2R model will be necessary, which subsequently leads to different path loss models from those obtained under the flat-earth assumption. 2) *Ducting effect:* Although the height of the transmitter is generally higher than the duct layer, part of the radio energy could still be trapped in the duct layer when the grazing angle (i.e., the angle between the direct path and the sea surface plane) is less than a

[3] In this paper, we use the term ''null'' to describe that the received signal strength meets sudden drop.

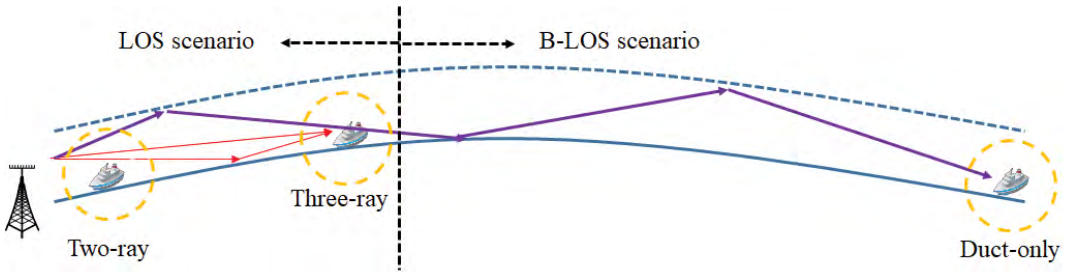

FIGURE 3. Illustration of the near-sea-surface channel links which are shown to be *location-dependant*.

certain threshold. In this case, the ray-trapping effect of the evaporation duct (and evaluated duct) will notably increase the energy of the received signals, resulting in path loss reduction. In measurements, the recorded path loss reduction could be up to 10 dB [37].

A general path loss model for the air-to-sea channels, following the classic logarithmic path loss model structure, was described in [38] as

$$PL(d)|_{dB} = PL\,(d_0) + 10n\log_{10}\left(\frac{d}{d_0}\right) + \chi_\sigma + \varsigma F, \quad (3)$$

where d_0 is the reference distance, n is the path loss exponent which could be *less than* 2 thanks to the ducting effect over the sea surface, and χ_σ describes the shadow fading. Note that although the presence of obstacles is expected to be rare, shadowing effect is still considered in (3) due to, e.g., sea waves in the condition of high sea state levels. To incorporate the fast moving of the aircraft-based transmitter, an adjustment parameter F is introduced, while ς is set to 1 or -1, depending on the moving direction of the aircraft (towards or away from the ground site). Measured values of these parameters for different scenarios and carrier frequency are referred to [38, Table VII].

2) ROOT MEAN SQUARE DELAY SPREAD (RMS-DS)

In the case that the air-to-sea channel is dominated by the two-ray components, the RMS-DS is usually small, especially for high aircraft altitudes [38]. When the third ray cannot be ignored, the RMS-DS of the air-to-sea channel will be significantly affected by the sea wave condition and the existence of the duct layer: First, as described in the previous subsection, higher sea state level may decrease the occurrence probability of the third ray in (1), and consequently, decreases the RMS-DS. Second, in the presence of the duct layer, additional rays may arrive at the receiver from small grazing angles, which may substantially increase the RMS-DS as compared to that measured inland.

In [36], measurements of the RMS-DS have been conducted for scenarios with or without the duct layer. The reported results have shown that 1) the duct-layer propagation leads to much larger RMS-DS for the reason that the trapped signals encounter multiple reflections and refractions; 2) the aircraft altitude plays an important role in determining the RMS-DS. A lower altitude leads to larger RMS-DS as the multiple reflection paths become more distinguishable; 3) the RMS-DS is also affected by the sea condition. According to the measurements, larger RMS-DS was observed in the calm sea conditions than that observed with rougher sea. The measurement result agrees with the previous discussion where it has been shown that a third propagation path is more likely to exist in the calm sea condition, which subsequently induces larger RMS-DS.

3) RICIAN K-FACTOR

As mentioned, Rician fading could be used to describe the small-scale fading characteristics of the air-to-sea channel in the rough sea conditions. For this case, it is necessary to understand the distribution of the Rician K-factor. In [38], it has been shown that the Rician K-factor in dB increases almost linearly with the link distance. Due to the sea wave movement, the Rician K-factor is actually random and its mean value and standard deviation have been measured for different frequency bands. For example, the mean value of 31 dB and standard deviation of 1.8 dB have been measured for the C-band signals, while the mean value of 12.7 dB and standard deviation of 1.2 dB have been reported for the L-band.

IV. NEAR-SEA-SURFACE CHANNELS

In this section, we focus on the channel links in the land-to-ship/ship-to-land and ship-to-ship communications, i.e., the near-sea-surface channels. Following a similar line of reasoning of Section III, we first introduce the physical propagation characteristics of these channel links and highlight the "location-dependant" feature. Furthermore, noticing that the B-LOS transmission is crucial in the near-sea-surface radio propagations due to the limited antenna heights and earth curvature, we will describe the modeling details for the B-LOS propagation in addition to the LOS propagation.

A. PHYSICAL PROPAGATION CHARACTERISTICS

For the air-to-sea channels, a key feature could be concluded as "angle-dependant". More specifically, the air-to-sea channel characteristics would be largely different for different grazing angles. As an example, the duct layer propagation only exists when the grazing angle is smaller than a certain threshold, thereby causing different path loss model and delay spread.

In contrast, the near-sea-surface wireless channel can be described as *"location-dependant"*. As illustrated in Fig. 3,

different channel models should be selected depending on the Tx-Rx distance. When the Tx-Rx distance is small, the channel could be modeled using the classic two-ray model [11], [27], [35], [44], [45], where the LOS and the surface reflection paths are the two most dominant components of the channel. As the distance increases, the first ray from the evaporation duct layer appears (if exists). In this case, the three-ray model provides a more precise description of the channel [30], [46]. If the receiver moves even farther away, both the LOS and the surface-reflection paths eventually vanish due to the earth curvature. However, the receiver can still receive signal in the presence of the duct layer, provided that the direction of the transmit beam is properly set. In conclusion, as the Tx-Rx distance increases, the propagation characteristic may change from two-ray to three-ray, and becomes duct-only in the end.[4]

According to Fig. 3, the propagation near the sea surface can be divided into two scenarios, namely LOS and B-LOS, where the former includes both the two-ray and three-ray propagations, and the latter is mainly due to the transhorizon propagation through the evaporation duct layer. In what follows, we discuss the channel modeling respectively for the LOS and B-LOS scenarios.[5]

B. LOS TRANSMISSION

LOS transmission is the most common communication scene of short-range maritime activities, including coastal traffic, coast guarding and near-sea fishery. The LOS path exists when the Tx-Rx distance is relatively short. Geometrically, the largest distance that can support LOS transmission can be calculated as [83]

$$d_{LOS} = \sqrt{h_t^2 + 2h_tR} + \sqrt{h_r^2 + 2h_rR}, \tag{4}$$

where h_t and h_r are the heights of the Tx and Rx antennas, respectively, and R is the Earth radius. For instance, the maximum LOS distance is approximately 35 km with antenna height 40 m. For ship-to-ship communications, this distance might be shorter due to the limited onboard antenna height. Many modeling approaches have been proposed to characterize the maritime LOS transmission. We summarize some major approaches in the following.

1) EMPIRICAL PATH LOSS MODELS

It is important to have an accurate large-scale path loss model so that the transmitter can set its power accordingly to support long-range maritime communications. For this purpose, one straightforward approach is to use the well-known empirical path loss models with necessary modification to fit the maritime environment. In this regard, the widely used Okumura-Hata model has been modified for the maritime environment in [84], which accounts for the sparse distribution of obstacles and scatterers in the wide open sea area. The irregular terrain methodology (ITM) model, a.k.a. the Longley Rice model [85], introduces extra physical parameters such as the sea wave conditions and the climates. In [39], it is shown to provide more precise results than the Okumura-Hata model. The ITM model has been further improved in [40] by including the impacts from the two-ray propagation and rain attenuation. Recently, the International Telecommunication Union (ITU) has proposed a path loss model ITU-R P.1546-5 [41]. The ITU model was intended for the use in tropospheric communications. It is applicable for many scenarios with antenna heights from 10 m to 3000 m, and supports transmission distance up to 1000 km. In [42], it has been shown that when the transmission distance is short, the above empirical models have similar performance. As the transmission distance increases, the ITU model is shown to be more consistent with measurements than the other models.

Consider the classic logarithmic path loss model structure, which is given by

$$PL(d) = PL(d_0) + 10n\log_{10}\left(\frac{d}{d_0}\right) + \chi_\sigma. \tag{5}$$

A number of campaigns have been conducted to measure the key parameters of (5) in the maritime environments, i.e., the path loss exponent n and the standard deviation σ of the log-normal distributed shadow fading factor χ_σ [27], [32]–[34], [43]. For the frequency band ranges from 5 to 8 GHz, which has been granted by the European Conference of Postal and Telecommunications Administrations (CEPT) and European Telecommunications Standards Institute (ETSI) to offer maritime broadband communications [83], [86], many recent measurements and modeling approaches have been reported, as summarized in Table 1.[6] Several important observations are highlighted as follows: 1) The path loss exponent varies quite differently in different scenarios. Besides the carrier frequency, other factors that would affect the value of n include the Tx/Rx antenna height, the link distance, and the existence of LOS path etc. 2) Albeit less shadowing effect was expected in maritime communications due to the sparse distribution of obstacles, it could still be described as log-normal distribution. The shadowing effect may be caused by the blocking reefs and passing-by vessels, and might also affected by the sea waves. In practice, higher sea state levels lead to larger value of σ.

In Table 1, it has been shown in [27], [32], and [43] that the two-ray model outperforms the classic logarithmic path loss models in describing the periodical oscillation shown in the measured signal strength, when the Tx-Rx distance is short and there exits a dominant LOS path. As such, the ray

[4]Note that the duct-only case does not mean that there is only one ray arrived through the duct layer. In fact, multiple rays encountering different times of reflections and refractions may arrive at the same Rx point, therefore resulting in a multipath fading channel.

[5]In the following, when the context is clear, we might use LOS to refer to the links that are *within the LOS range, i.e., not transhorizon* (even if there is no actual LOS path between the nodes due to blocking).

[6]In Table 1, NLOS specifically refers to the scenarios that the Tx-Rx distance is *within the LOS range* (i.e., $d < d_{LOS}$ in (4)), while the actual LOS path is blocked by obstacles.

TABLE 1. Recently reported logarithmic path loss model parameters for maritime LOS transmission.

Freq. (GHz)	Ref.	Max Meas. Dist. (km)	n	σ	Scenario	Tx/Rx Ant. Heights
5.8	[33]	10	4.5768	3.489	Buoy-to-ship (LOS)	1.7/9.8
			2.0790	5.1224	– (NLOS)	
			4.2923	7.1520	– (Mixed LOS/NLOS)	
	[34]	10	5.6	6.4	Buoy-to-ship	1.9/9.8
			2.7	4.9	Buoy-to-boat	1.9/2.7
			3.4	5.5	Buoy-to-land	1.9/5.45
	[43][1]	7	2.165	3.69	Land-to-boat (Moving)	185/8
			2.161	4	– (Drifting)	
		20	2.35	7.86	– (Moving)	76/8
			2.29	5.47	– (Drifting)	
		18	2.39/6.12	8.4	– (Moving)	4/8
			2.38/7.57	8.7	– (Drifting)	
5.2	[32][2]	1.9	2.48	4.2	Ship-to-land (LOS)	7.95/32.9
			3.6	4.4	– (NLOS)	
			4	4.4	– (NLOS)	7.95/21.6
2.4	[27][3]	2	2.09/1.96	3.24/3.28	Land-to-ship (LOS)	3/4.5

[1] It has been demonstrated that the two-ray model has better fit to the measurement in the conditions with a dominant LOS path. Moreover, for the third case (Tx/Rx antenna heights being $4/8$), a double sloped path loss curve is observed. Therefore, two path loss exponents are obtained respectively for these two slopes.
[2] Oscillation in the received power is observed in the distance range of $(650m, 800m)$, due to the destructive summation of the LOS path and surface-reflected path.
[3] Two sets of parameters (n and σ) are obtained by fitting the measured data respectively to the floating intercept path loss model and the close-in reference path loss model. However, a modified two-ray model is found to be more accurate than these logarithmic path loss models.

trajectory-based path loss models, including both the two-ray and a three-ray model, are introduced in the following.

2) TWO-RAY AND THREE-RAY PATH LOSS MODELS

Although the empirical path loss models can efficiently predict the *average* signal strength in the maritime environment, they fail to fit the *local oscillations* resulted from the destructive summation of sparse multipath signals. To address this problem, the ray trajectory-based path loss models geometrically identify the trajectories of the most dominant rays arrived at the receiver. Accordingly, the phase shift of each ray is characterized and considered in the path loss calculation, therefore providing a better description of the local peaks and nulls of the received signal strength.

Using the two-ray model, the path loss in dB at distance d can be calculated as [30, eq. (2)]

$$L(h_t, h_r, d) = -10\log_{10}\left(\left(\frac{\lambda}{4\pi d}\right)^2\left(2\sin\left(\frac{2\pi}{\lambda}\frac{h_t h_r}{d}\right)\right)^2\right), \quad (6)$$

where h_t and h_r are the Tx and Rx antenna heights, respectively, and λ is the carrier wavelength. For the near-sea-surface LOS propagation, the two-ray path loss model is accurate as shown by a number of measurement campaigns using various carrier frequencies and transmission protocols [11], [45], [74]. It has been shown that the deep nulls calculated from (6) well match with the measured data especially for the offshore environment [27], [32], i.e., when the Tx-Rx distance is relatively short. According to the two-ray model, deep nulls in the received signal strength periodically appear as the Tx-Rx distance increases, and a maximum variation up to 60 dB was observed between peaks and nulls [9].

Note that deep nulls calculated from (6) only appear within the distance range (d_0, d_{break}) where $d_0 = h_t$ and $d_{break} = \frac{4h_r h_t}{\lambda}$ [30]. The reasons are: 1) The received signal strength of a receiver whose distance is less than d_0 will be increasing since the signals from the two paths will always be constructively combined; and 2) when the distance is larger than d_{break}, the signal strength would monotonously decrease as the two-ray signals will always be destructively combined. However, measurements have shown that deep nulls still exist when the distance is larger than d_{break} [30], [46]. This suggests the possible existence of an additional path. In [30], it is conjectured that a third ray might come from the trapped

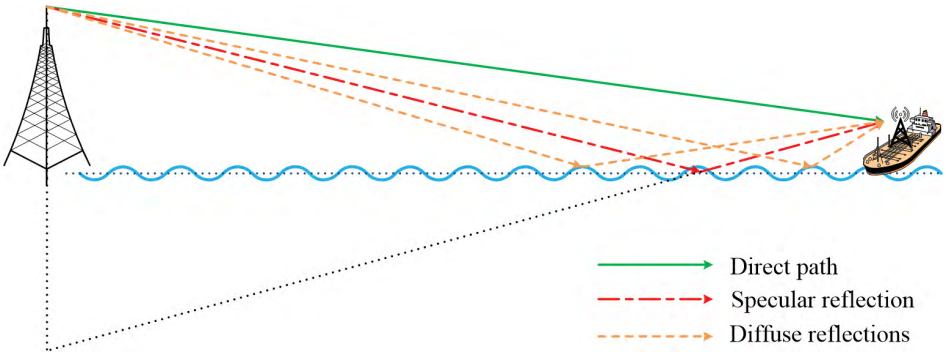

FIGURE 4. Illustration of the direct, specular, and diffusion reflection paths in the near-sea-surface propagation (reproduced from [47, Fig. 1]).

signals in the evaporation duct layer. In this case, the three-ray path loss model is given by

$$L(h_t, h_r, h_e, d) = -10\log_{10}\left(\left(\frac{\lambda}{4\pi d}\right)^2 (2(1+\Delta))^2\right), \quad (7)$$

where $\Delta = 2\sin\left(\frac{2\pi h_t h_r}{\lambda d}\right)\sin\left(\frac{2\pi(h_e-h_t)(h_e-h_r)}{\lambda d}\right)$ and h_e is the effective height of the evaporation duct. The three-ray model is shown to fit the measured results quite well for $d > d_{break}$ where the two-ray model fails to predict the null locations in this region [30].

The existence of the third ray relies on various factors including the Tx/Rx antenna heights, the evaporation duct height, as well as the refractivity of the atmosphere. Given these parameters, the distance beyond which that the third ray may appear can be determined via the ray tracing methods [52]. Approximately, for the near-sea-surface LOS transmission, the deep nulls in the received signal strength can be well predicted by simply applying the two-ray path loss model in the range of $(0, d_{break})$, and then apply the three-ray model in the range of (d_{break}, d_{LOS}).

3) SMALL-SCALE FADINGS

In addition to the dominant paths considered in (6) and (7), there may also exist multiple weak paths similar to those in the air-to-sea channels. These weak multipaths introduce more randomness, which need to be considered when describing the small-scale fading of the channel.

An important source of these weak multipaths is the multiple reflections from the rough sea surface. As shown in Fig. 4, when calculating the large-scale path loss in (6) and (7), only the specular reflection path is considered under the ideal assumption, i.e., calm sea surface. In practice, rough sea surface will produce more diffusion paths stemming from a sizable surface region (denoted as the *glistening surface* in [47]). The glistening surface can be modeled as the combination of a number of small mirror-like surfaces with random orientations (e.g., the angles of the reflections can be modeled as Gaussian distributed) [47]. The amplitudes of these diffusion paths can be characterized with the aid of the Karasawa's model as in [31, eqs. (1) and (2)]. On the other hand, the contribution to the weak multipath components from local scatterers such as the ship hull and surrounding objects cannot be neglected neither. Depending on the scenarios, the local scatterers could be assumed to be randomly distributed on the surface of a hemispheroid around the receiver.

By exploiting the propagation geometry and stochastically characterizing all the scattered paths with their angles of departure and arrival (i.e., AOD and AOA), amplitudes and delays, the classic GBSMs can be used to model the physical radio propagation [87]. However, when the number of multipath components is large, the conventional GBSMs are not efficient for the theoretical analysis. Recently, the so-called two wave with diffusion power (TWDP) model has drawn attentions in the modeling of mmWave channels where the dominant paths are sparse. The TWDP model simplifies the conventional GBSMs by replacing multiple weak paths with a single diffusion term, described as [66, eq. (4)]

$$\tilde{V} = \sum_{i=1}^{N} V_i \exp(j\Phi_i) + X + jY, \quad (8)$$

where $N = 2$. $\tilde{V}$ is the total voltage induced at the receive antenna consisting of two parts: the specular component $\sum_{i=1}^{N} V_i \exp(j\Phi_i)$, and the diffusion part $X+jY$ which follows complex Gaussian distribution and represents the sum of numerous independent weak waves. The TWDP model is inherently appropriate for modeling the maritime LOS propagation, especially for the high sea state levels: the specular component in (8) corresponds to the combination of the direct path ($i = 1$) and the specular reflection path ($i = 2$) in Fig. 4; the diffusion term corresponds to the randomness induced by multiple weak paths from rough sea surface reflections and/or rich local scattering. Compared to the conventional GBSMs, the TWDP model provides a tractable analytical form for the maritime LOS channel. Although the probability density function (PDF) of (8) is not available in closed-form, close approximations which enable fast numerical evaluations can be found [66].

Note that both V_1 and V_2 in (8) might be fluctuating too, and should be considered as random in some conditions

(In the maritime environment, this might be caused by waves). In this regards, the TWDP model is generalized to the fluctuating two-ray (FTR) model in [67] and [68]. The FTR model has several advantages: Its PDF can be derived in closed-form, and the model can be reduced to well-known distributions (e.g., Rician or Rayleigh) in certain conditions. For example, as the Tx-Rx distance increases, the LOS path and the dominant reflection path tend to have similar path length, and the phase difference between these two paths approximately stays unchanged. In this scenario, these two paths can be combined as one. Note that the randomness caused by the specular part and the diffusion part in (8) have different time scales, where the former will encounter a much slower changing rate. Therefore, during a short period where the specular component is fixed, the overall small-scale fading simply reduced to Rician. In the maritime environment, the match between the Rician fading and measurements has been confirmed in [27], [29], and [50] for different carrier frequencies and Tx-Rx distances.[7]

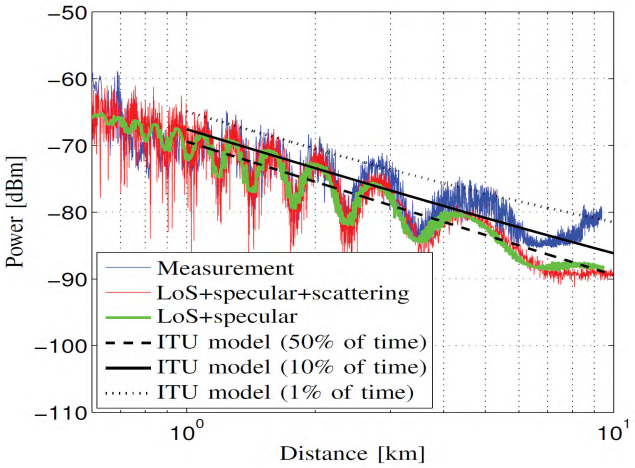

FIGURE 5. Received power vs. Tx-Rx distance in a maritime LOS environment [31, Fig. 7]. Measurements are compared with the empirical path loss model (ITU), the two-ray model (LOS + Specular) and the specular + scattering models. *Parameters setting* – Carrier frequency: 5.2 GHz; bandwidth: 100 MHz; transmit power: 47 dBm; Tx antenna height: onboard, ∼7 m; Rx antenna height: 32.9 m.

As a conclusion of this subsection, we reproduce [31, Fig. 7] as Fig. 5 to show the relations and the applicable scenarios of the introduced large- and small-scale channel models. As shown in the figure, the measured channel shows significant oscillations due to the destructive combination of the direct and the specular reflection waves. The empirical ITU model can be used to describe the large-scale decaying in the average received signal power, but it fails to identify the null locations. A two-ray path loss model incorporating the LOS path and the specular reflection path accurately fits the location-dependent null points, but the small-scale fading caused by the diffuse multipath components is not characterized. By further introducing a scattering component to the two-ray model, the simulated curve shows the best fit to the measurements.

[7]Note that except for the Rician fading, some other fits have been reported in the literature, depending on the specific propagation environment (with or without actual LOS path etc.). For instance, in [34], the small-scale fading, when expressed in dB, is shown to fit well with the extreme value distribution.

C. B-LOS TRANSMISSION

B-LOS transmission is possible in maritime communications thanks to the ducting effect over the sea surface. As a promising approach to achieve long-distance and high security transmission, B-LOS transmission using the ducting effect has attracted much attention in military communications. For X-band signals, the communication range can be dramatically extended to up to 1000 km with the aid of the duct layer [53].

In the previous subsection, it has been shown that a third ray from the duct layer may introduce additional nulls in the received signal strength. As illustrated in Fig. 3, when the LOS and reflection paths vanish at long Tx-Rx distance, i.e., beyond d_{LOS}, the wireless channel solely relies on the radio propagation in the duct layer. To better understand the maritime B-LOS channel, wave propagation tools have been widely used, e.g., the AREPS and PETOOL [52], to solve the parabolic equation (PE) approximation of the Helmholtz wave equation by numerical means [52], [88]. The path loss can be obtained accordingly with the solution of the PEs. The fundamental theory of the PE method and a series of its applications can be found in [88]–[91]. Although the PE method can efficiently solve the electromagnetic propagation problem and estimate the field strength at any interested location, it cannot describe the propagation characteristics in the spatial or delay domain, i.e., the AOA/AOD and the delay spread. To address this problem, the ray optics (RO) method, a.k.a. optical ray tracing (ORT), is introduced to find the trajectory of each ray by solving the Snell's equation [89], [92], [93]. The ORT method reveals more propagation details at a cost of higher computational complexity. In practice, the PE and ORT methods can be combined to provide a more precise description of the channel [94], [95].

Several key features have been reported for maritime B-LOS channel via measurements or simulations: 1) The capability of B-LOS transmission relies on the carrier frequency, where it has been shown that the X-band is preferable. In [61], the researchers have established a high-speed B-LOS microwave link operating at 10.5 GHz in Australia, and a path loss of 141 dB was recorded at the distance of 80 km, while the C-band (4-8 GHz) signals experienced about 30 dB higher path loss at the same distance. This phenomenon has also been confirmed by the simulations using the PETOOL. 2) Only the transmission within a certain angle range, i.e., the trapping beamwidth as denoted in [52], can be trapped in the duct layer, while radio waves emitted outside of this range will spread in the atmosphere. The maximum and minimum trapping angles are symmetric and are given by [52] and [96, eq. (5)]

$$\theta^T_{\max/\min} = \pm\sqrt{2\left(\frac{1}{n(0)}\frac{\partial n}{\partial z}+\frac{1}{R}\right)(h_t-h_e)}, \qquad (9)$$

where n is the atmospheric refractive index, which is a function of z, the vertical height. $n(0)$ is a reference constant value, R is the earth radius, h_t and h_e are the heights of the Tx antenna and the duct layer, respectively. With $h_t = 27$ m and $h_e = 40$ m, the calculated trapping angles are very narrow ($\pm 0.266°$) [52], which would impose high requirement on the Tx beamforming design.

In the next, we follow a similar structure as the last subsection and continue to introduce the large- and small-scale fadings in the B-LOS channel.

1) PATH LOSS MODELS

As the Tx-Rx distance increases and is beyond the clearance of the first Fresnel zone, the received signal strength will have sudden drop even if the LOS path exists, i.e., $d < d_{LOS}$. As shown in Fig. 6, the ITU model well matches with the measured data and still maintains its accuracy for the transhorizon propagation, while both the free space and two-ray models overestimate the received power in this region [83]. Note that the water temperature at the time of measurement was only 6°C, and it is unlikely that there exists evaporation duct. In this case, the path loss in the transhorizon region is much higher than that of the free space.

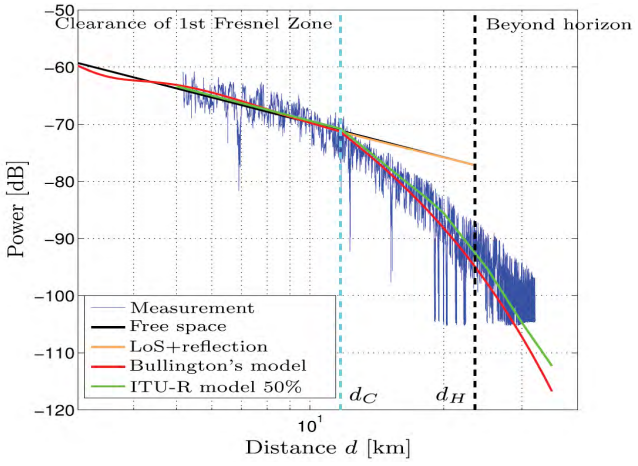

FIGURE 6. Measured path loss compared with the theoretical and empirical models [83, Fig. 5]. Obvious decreasing in the received signal strength is observed beyond the clearance of the 1st Fresnel zone. ***Parameters setting*** – Carrier frequency: 5.2 GHz; bandwidth: 120 MHz; transmit power: ∼43 dBm; Tx antenna height: onboard, ∼16 m; Rx antenna height: 6 m.

In the presence of evaporation duct, the path loss might be lower than that of free space thanks to the wave trapping effect. Under the ideal assumption with uniformly distributed duct layer (i.e., constant layer height) and flat sea surface, the path loss exponent was calculated using the PETOOL as 1.2087 in [53]. The value is smaller than 2 (the free space exponent) since the trapping effect of the duct layer prevents the signal power from spreading through the atmosphere.

In contrast to the ideal assumptions, the refraction conditions of the duct layer are not uniform and range-dependant in practice. Besides, the sea surface is rough according to the realistic sea wave conditions. These lead to a higher actual path loss exponent than the theoretical value [53], and it is random rather than constant. Dinc and Akan [52] obtained the parameters of the logarithmic path loss model in (5) based on the PETOOL. Taking practical parameters such as the the Tx height (h_t), Rx height (h_r), duct height (h_e), duct strength (Δm), and carrier frequency (f) into consideration, the parameters are given by [52, eq. (22)]

$$PL(d_0) = \alpha_A + \beta_A \Delta h + \kappa_A h_e + \xi_A f + \rho_A \Delta m + \sigma_{\Delta A} x,$$
$$n = \alpha_n + \xi_n f^2 + \rho_n \Delta m + \sigma_{\Delta n} y,$$

where $\Delta h = |h_t - h_r|$, and $\alpha, \beta, \kappa, \xi, \sigma$ are the coefficients obtained via multivariate regression analysis. Note that the randomness is introduced to the path loss parameters via x and y, which are random Gaussian variables with zero mean and unit variance. Besides, it was concluded that the shadow fading (in dB) in the ducting propagation best fits the log-Weibull distribution, whose parameters can be similarly obtained through the regression analysis.

Measurements of the path loss in the evaporation duct layer have been conducted recently. In [97], the path loss exponent value of 2.1 was observed for 10.4 GHz carrier frequency, which is slightly higher than the free space path loss. In [98], the path loss is modeled as the free space path loss multiplied by a modification factor. It has been shown in [98, Fig. 13] that when the Tx-Rx distance is relatively short, the measured signal strength decreases following a similar trend of the free space path loss model, while larger path loss is observed as the receiver goes farther. Although the trapping effect provided by the ducting transmission is expected to enhance the received power, practical measurements have revealed that additional losses might be induced by unideal factors such as the low reflection coefficient caused by rough sea surface, and by the refraction loss caused by non-uniform duct layer distribution. A thorough review of recent measurement achievements and analysis is referred to [98].

2) SMALL-SCALE FADINGS

To understand the small-scale fading in maritime B-LOS channel, it is necessary to first characterize the multipath propagation within the duct layer. For this purpose, the ORT method is preferred to estimate the possible arrived rays at a given point.[8] By approximating the electromagnetic propagation in different directions with distinguishable rays, the ORT method is able to simulate the channel by summing up all the incoming rays at a given location. A Matlab-based ray-tracing package is referred to [99], while the model relies on some ideal assumptions such as range-independent refractivity. Zhao and Yang [51] designed a 2D visualization ray tracking tool (Ray-VT) to capture the realistic environment factors including range-dependent refractivity and arbitrary

[8] As a deterministic modeling technique, ORT is usually used as a counterpart to the PE method to characterize the field strength in a given environment. Nevertheless, we introduce the ORT method in this subsection since it can provide the information of the propagation geometry, required by other conventional physical channel models to model the small-scale fading.

terrains. The proposed ORT method was compared with the PE-based approaches. While the consistency has been shown in the field strength distribution, the ORT method can additionally provide information on the possible ray trajectories between the transmitter and receiver, and correspondingly, the AOAs/AODs and delay spreads. Detailed comparisons between the ORT- and PE-based methods can be found in [89].

The fundamental theory of ORT is referred to early contributions such as [100], and it has been specifically modified for the maritime B-LOS propagation modeling in [101]. Instead of going into the details of the ORT method, we focus on the channel statistics of the B-LOS duct channel, and highlight a few key conclusions obtained using ORT in the following.

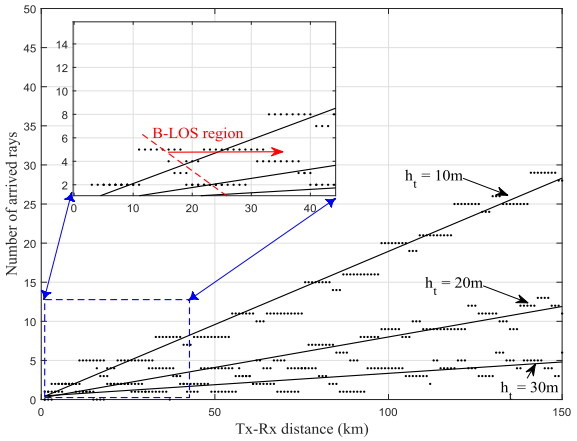

FIGURE 7. Number of arrived paths vs. the Tx-Rx distance (obtained using ORT simulations). *Parameters setting* – Carrier frequency: 10 GHz; Tx antenna height: 10/20/30 m; Rx antenna height: 20 m; duct layer height: 40 m.

One important feature for the duct layer propagation is the number of multipaths increases almost linearly with the Tx-Rx distance as shown in Fig. 7. When the Tx-Rx distance is short, there exists only a limited number of multipath components. From the perspective of physical propagation, different approaches can be used to describe the small-scale fading of the channel, here we list two typical ones: 1) The classic GBSM-based model structure can be applied if the transmission geometry is known [87]. 2) The extended Saleh-Valenzuela (S-V) model can be used without the needing to know the exact transmission geometry [65]. It only requires the information on some physical parameters such as the AOA/AOD, delay, and the complex gain of each multipath component, while the distribution of these parameters can be modeled with the aid of results obtained using ORT. For example, it is known that the AODs will be distributed within the trapping beamwidth, which can be determined using the ORT method. Note that the extended S-V model has recently attracted attentions in the research of mmWave communications [102], which experiences sparse channels similar to that in the maritime environment.

From the statistical modeling perspective, when the Tx-Rx distance is just beyond d_{LOS}, there may exist one dominant path along with multiple weak paths. For this case, recent measurements have observed that the corresponding small-scale fading can be simply modeled by Rician distribution [103]. On the other hand, the number of multipath components becomes large as the distance increases as shown in Fig. 7. In systems that the chip period is comparable to the delay spread, all these paths will be combined together, and the small-scale fading can be simply approximated by Rayleigh distribution when the Tx-Rx distance is large. The converge to Rayleigh is confirmed by our ORT simulation as shown in Fig. 8.

D. OTHER KEY PARAMETERS OF THE NEAR-SEA-SURFACE LOS/B-LOS CHANNELS

In this subsection, we summarize some other important parameters for the near-sea-surface LOS/B-LOS channels reported in the literature, including the Rician K-factor, the delay spread and frequency spread (coherence time). In what follows we list some most recent results obtained from either measurements or stochastic modeling approaches.

As described, the Rician fading can be used to describe the small-scale fading for either the LOS or B-LOS propagations when there exists dominant paths. The Rician K-factor has been investigated in [29], [83], and [104]. It was shown that the measured Rician K-factor is influenced by the antenna heights, where higher antenna leads to smaller mean value and deviation of the K-factor [29]. Besides, the K-factor decreases with the Tx-Rx distance. In particular, when the distance is beyond the first Fresnel zone, the K-factor substantially decreases due to the blocking of the LOS path (see Fig. 6). For the B-LOS propagation, the Rician K-factor keeps decreasing as the distance increases and finally the channel becomes Rayleigh [83]. This observation agrees with the results in [98], and can also be explained by using the ORT method as shown in Fig. 7 and Fig. 8.

Results on the delay spread have been reported for the maritime LOS channels in [28], [46], and [105]. It has been shown that the delay characteristics depend on various factors including the carrier frequency, the scattering environment, and the sea wave conditions. In [28], a maximum resolvable delay of 10.24 μs is observed for 2.075 GHz signals in an open sea area ranges from 3 to 12 km. Stochastic ray method was applied to investigate the statistical characteristics of the multipath propagation in [49], and the mean excess delay of 8.95 μs and RMS-DS of 9.64 μs were reported. For the 5.8 GHz carrier frequency, the mean delay of 61 ns and RMS-DS of 183 ns were recorded in a sea port scenario [105].

At last, due to the sparse nature of maritime radio propagations, the frequency spread is found to be very narrow for both the LOS and B-LOS transmissions. In [28], the Doppler shift was shown to be only 0.16 Hz with carrier frequency 2 GHz. The coherence time for the B-LOS ducting propagation was investigated in [54]. It was observed that the frequency spread

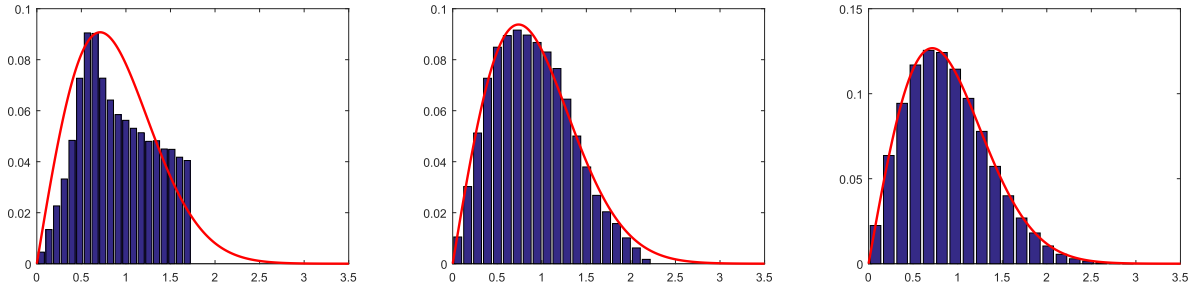

FIGURE 8. Rayleigh distribution fit to the simulated channel samples at different Tx-Rx distances. (a) 60km. (b) 100km. (c) 500km.

in the duct channel is also limited due to the narrow trapping beamwidth, and a coherence time up to 2.9 ms has been reported for carrier frequency of 10.5 GHz.

V. KEY FEATURES OF THE MARITIME WIRELESS CHANNELS

In this section, we summarize the two most important features of the maritime wireless channels: *sparse* and *location-dependant*.

A. SPARSITY

The sparse property holds for both the air-to-sea and near-sea-surface channels. Sparsity is seen in three aspects: 1) Sparse distribution of multipath components (MPCs), 2) sparse distribution of AOAs/AODs, and 3) sparse distribution of user locations.

For the first aspect, according to the number of MPCs that being considered, the applicable channel models are summarized as follows:

- *Hybrid two-ray/three-ray models:* The two-ray model only considers the LOS path and a specular reflection path as two dominant MPCs of the channel. By introducing a third ray, the three-ray model could be used to describe the air-to-sea channel when the sea surface is rough, and may also be used to describe the near-sea-surface channel in the distance range (d_{break}, d_{LOS}). Depending on the application, the two-ray or three-ray assumption might have different expressions in practice, e.g., the tapped delay line models in (1) and (2), and the ray trajectory-based path loss models in (6) and (7).
  With calm sea surface, the two-ray and three-ray models are accurate in describing the large-scale path loss. However, they consider only two or three major rays and omit other possible weak MPCs. This makes the two-ray and three-ray models inaccurate in describing the small-scale fading in maritime channels.
- *TWDP/FTR models:* In addition to the two dominant paths in the two-ray model, the TWDP/FTR models introduce an additional component to describe the diffusion power caused by multiple weak paths. In the maritime environment, these paths stem from rough sea surface reflection and/or scattering from local scatterers. The TWDP/FTR model would reduce to the Rician or Rayleigh fading in certain conditions.
- *Physical models with sparsely distributed MPCs:* In some conditions, the TWDP/FTR models cannot be applied for the reasons that: 1) There lacks of dominant paths; and 2) the amount of diffusion multipaths is small so that their combination cannot be properly described by a known distribution. In this case, the physical models, such as the GBSMs and the extended S-V model, could be adopted if the transmission geometry or the distribution of physical parameters such as the AOA/AOD are known.
  One example is the near-sea-surface B-LOS channel when the Tx-Rx distance is just beyond d_{LOS}: The two-wave component does not exist because the transmission is transhorizon, and the number of MPCs is small as illustrated in Fig. 7. While the transmission geometry can be characterized with the aid of the ORT method, GBSM-based models can be applied to describe the fading characteristics for this scenario. Note that as the number of arrived paths increases with the distance, the small-scale fading of the channel will eventually converge to the Rayleigh distribution.

Sparsity is also seen in the angle domain: 1) For the LOS propagation, multipaths might be caused by the rough sea surface reflections. Despite that the number of multipaths could be large when the sea state level is high, these paths mainly come from similar angular directions; 2) for the B-LOS propagation, the trapping beamwidth is usually very narrow as described in (9). The angular sparsity will induce high correlation between the adjacent antenna elements in maritime wireless MIMO channels.

At last, the maritime users are usually sparsely distributed. Such sparsity means that the users at different locations may encounter largely different path losses. The largely dispersed path loss distribution is caused not only by the Tx-Rx distances, but also by the deep nulls resulted from destructive summations of the two or three dominant paths as shown in (6) and (7).

TABLE 2. Large- and small-scale near-sea-surface channel models according to the Tx-Rx distance.

Tx-Rx distance		LOS ($d < d_{LOS}$)		B-LOS ($d > d_{LOS}$)	
		$d < d_{break}$	$d > d_{break}$	near[3]	far
Large-scale	Empirical	ITU [41]/ITM [40]			
	Ray trajectory-based	Two-ray	Three-ray	ORT models (combined with PE methods)	
Small-scale	Physical[1]	TWDP [66]/FTR [68]	GBSM-based models/Extended S-V model		
	Statistical	Rician/Rayleigh[2]		Rayleigh	

[1] The physical channel models require physical description of the propagation, such as the transmission geometry or the AOAs/AODs. Here the TWDP/FTR models are categorized as physical models since the two-wave component depends on the physical propagation of the LOS and the specular reflection paths.

[2] The distribution could be either Rayleigh or Rician in the high sea-state-level scenarios, depending on whether there exists a direct path.

[3] There is no explicit break point between "near" and "far", and this partition is based on empirical results: On one hand, Rayleigh distribution is possible at far distances as shown in Fig. 8; on the other hand, Rician fading was observed in the range just beyond d_{LOS} in the measurements [103].

B. THE LOCATION-DEPENDANT FEATURE

In the maritime environment, different user location may lead to totally different model structure, which differentiates from that inland where usually only the path loss is affected. To be specific, the important location-dependant parameters are the grazing angle in the air-to-sea channels, and the Tx-Rx distance in the near-sea-surface channels.

With large grazing angle, the air-to-sea channel can be described by the two-ray model for calm sea surface, and described by the three-ray model when the sea surface is rough. When the grazing angle becomes smaller, the wave could be trapped in the duct layer and encounter multiple reflections and refractions in the long-distance propagation. In this case, the GBSM or the extended S-V models are preferable since they can incorporate the effects of more rays propagated through the duct layer.

For the near-sea-surface propagation, we recall Fig. 3 and list the appropriate channel models for three typical scenarios with different Tx-Rx distance ranges, respectively, as follows:

- *LOS Propagation for $d < d_{break}$:* With calm sea surface, the two-ray model can be used to model the large-scale path loss and identify the deep-null locations in the channel link. The two rays correspond to the LOS propagation and the specular reflection paths, respectively. When the sea state level is high, the rough sea surface induces more scattering and reflections, and the TWDP/FTR models provide a good structure to capture the small-scale fading characteristics of the channel.
- *LOS Propagation for $d \in (d_{break}, d_{LOS})$:* As the Tx-Rx distance increases, three major rays exist in this range, i.e., the LOS, the specular, and the ray through the duct layer. For the large-scale fading, the three-ray path loss model could be used. For the small-scale fading, the TWDP/FTR models are not applicable anymore as there exits more than two dominant rays. Instead, the physical models (GBSMs or extended S-V) can be applied.
- *B-LOS Propagation for $d > d_{LOS}$:* For the B-LOS propagation, the path loss in a deterministic environment can be characterized using the ORT/PE methods. For the stochastic channel modeling, GBSM-based models could be applied if the propagation geometry is known, which can be obtained with the aid of ORT. Note that the number of arrived rays increases with the Tx-Rx distance as demonstrated in Fig. 7. As a result, the fading distribution can be described as Rician when there exists a dominant path (possibly in a short distance range that is just beyond d_{LOS}), and eventually converges to Rayleigh at far distance.

To summarize, we list the introduced channel modeling approaches according to their applicable distance range in Table 2. Note that these models could be jointly used to provide a better description of the realistic channel. For example, the empirical ITU path loss model has been combined with a two-ray component to describe the large-scale fading in the harbor environment in [106].

VI. FUTURE RESEARCH TOPICS IN MARITIME WIRELESS CHANNELS

In this section, we discuss the future research topics from the following two aspects: 1) The impacts of channel features in maritime communication system design, and 2) the development of more sophisticated maritime channel models.

A. IMPACTS OF MARITIME CHANNELS IN COMMUNICATION DESIGN

In the maritime environment, it may face more challenges in communication design than the terrestrial systems. First, in order to guarantee long-distance communications, channel state information (CSI) of the intended user is necessary for the transmitter to properly concentrate its power. Accurate and prompt CSI acquisition could be difficult in maritime communications due to 1) large feedback delay caused by long Tx-Rx distance, and 2) poor channel condition caused by link mismatch, deep nulls, and high path loss.

To address the feedback problem, statistical and outdated CSI-aided transmission schemes could be applied in maritime communications [107], [108]; to improve the channel estimation performance, the sparsity feature of the channel can be exploited to concentrate the resource only on the channel's dominant components. Besides the instantaneous CSI, the location information can be conveniently obtained in maritime communication systems, thanks to the implementation of the AIS system which regularly updates the vessels' locations at the central controller. Recalling that the maritime channels are location-dependant and the vessels move slowly, the location information is especially important and can be utilized in long-term CSI based transmission design. Liu *et al.* [109] creatively utilized the location-based large-scale CSI to design hybrid precoding, power allocation, and user scheduling strategy, which have opened up a new direction for maritime communication system design.

When the CSI is known, beamforming can be used to concentrate power towards the intended user with multiple antennas deployed at the transmitter [110]. However, channel sparsity in the angle domain brings challenges in the beamformer design. As an example, the trapping beamwidth was shown to be less than 1° for the duct layer propagations in some conditions. In this case, a narrow beamformer suffers from poor robust stability, since a sight error in the estimated trapping beamwidth may lead to severe power spreading out of the duct layer. In contrast, a wide beamformer could be more robust but at the cost of low trapping efficiency (i.e., the ratio between the wireless power that being trapped in the duct layer, and the total power emitted from the transmitter), which may reduce the coverage. Optimal beamwidth is to be designed to find the best tradeoff between these opposite effects.

New design problems also arise at higher layers and some examples are described in the following: 1) Due to the sparse user distribution in the marine environment, the channel conditions of different users vary quite differently. How to guarantee fairness in the user scheduling could be a key challenge in this scenario. Another important issue should be concerned is that for a far user, the communication link cannot be established unless a beam has already been scheduled to the user's direction. This indicates that the scheduling has to be designed with only limited information of the user, e.g., the location information acquired from external sources such as the AIS system. 2) The large delay caused by long-distance transmission suggests that the amount of feedback in the transmission protocols should be minimized, otherwise it may lead to unaffordable transmission and processing delays. In this light, feedback-free higher layer techniques such as network coding could be a promising technique for maritime communications [111]. 3) Sparse user distribution and highly dynamic channels raise requirement on the design of new network architecture. Candidates such as the mesh network could provide reliable and flexible connections among the widely dispersed users. Affected by adverse factors such as channel instability, unexpected null locations, and limited CSI acquisition, the routing design in a maritime mesh network could be an important research direction.

B. DEVELOPMENT OF NOVEL MARITIME CHANNEL MODELS

Another research direction is to develop more sophisticated maritime wireless channel models. According to the literature review, most existing measurements and modeling approaches are based on the single antenna setup. When MIMO system is deployed, the modeling of spatial channel properties (e.g., the spatial correlation between adjacent antennas, the eigenvalue distribution in a MIMO channel matrix) is important. However, these still need further investigation in the maritime environment. Furthermore, it is anticipated that the massive MIMO technology could be used to support long-distance maritime communications, thanks to its ability of forming very sharp beam towards the intended direction [109]. Due to the large array size, the far field assumption usually adopted in conventional MIMO channel models may become invalid for massive MIMO channel modeling [112], [113]. However, in maritime massive MIMO channels where the Tx-Rx distance is extremely large, the availability of this assumption needs to be reconsidered. A massive MIMO channel measurement campaign is in progress recently in Norway, under the research project "LTE, WIFI and 5G Massive MIMO Communications in Maritime Propagation Environments (MAMIME)" [25]. Detailed measurement results are yet to be presented. Besides extending the maritime channel models to the MIMO/massive MIMO setup, measurements and modeling approaches on new frequency bands, such as the mmWave bands, have also attracted research attentions recently [114]–[116]. Moreover, note that the underwater communications also constitute an important part of future maritime communication networks. The modeling of the underwater channel is another important direction with the development of new underwater communication techniques.

Another promising direction for the maritime channel modeling is to design efficient channel generator/simulator. The maritime propagation environment is in general highly dynamic and complicated. The channel could be affected by many unexpected factors, such as the sea wave movement, refraction in the atmosphere, and non-uniform weather distribution in the vast sea area. As a result, it is usually difficult to precisely describe the maritime wireless channel and simplifications are inevitable. A simplified channel model could ease the analysis, however, it may also lead to inaccuracy in the performance evaluation. It is desired to validate the system performance in realistic maritime channels, yet, practical maritime channel measurement is usually costly. According to the recent progress in deep learning and artificial intelligence (AI), a generative adversarial net (GAN) could be used to simulate the channel effects after trained with a few real data [117]. It is expected that the AI-aided modeling approaches can be applied in the maritime environment, when

explicit mathematical description of the channel does not exist.

VII. CONCLUSIONS

In this paper, we have performed a detailed review of the modeling approaches and measurement achievements for the maritime wireless channels, including both the air-to-sea and near-sea-surface channel links. Existing results in the literature have been summarized from the perspectives of the large-scale path loss, small-scale fading, as well as other important channel parameters such as the Rician K-factor and the delay spread. From the reviewed literature, we concluded that the two most distinctive features of the maritime wireless channels can be summarized as sparse and location-dependant. Specific to these unique features, we further discuss their possible impacts and corresponding challenges that being raised to maritime communications design. Moreover, we discuss on the development of more sophisticated maritime wireless channel models as an outlook of future research directions.

REFERENCES

[1] A. Jennings, *Modern Maritime Communications*, document ITU-R WRS 16, ITU World Radiocommun. Seminar, Geneva, Switzerland, Dec. 2016. [Online] Available: https://www.itu.int/dms_pub/itu-r/md/15/wrs16/sp/R15-WRS16-SP-0026!!PDF-E.pdf

[2] G. D. Lees, *Handbook for Marine Radio Communication*, 6th ed. London, U.K.: Taylor & Francis, 2017.

[3] D. Kidston and T. Kunz, "Challenges and opportunities in managing maritime networks," *IEEE Commun. Mag.*, vol. 46, no. 10, pp. 162–168, Oct. 2008.

[4] W. Du, M. Zhengxin, Y. Bai, C. Shen, B. Chen, and Y. Zhou, "Integrated wireless networking architecture for maritime communications," in *Proc. 11th ACIS Int. Conf. Softw. Eng., Artif. Intell., Netw. Parallel/Distrib. Comput.*, London, U.K., Jun. 2010, pp. 134–138.

[5] M.-T. Zhou and H. Harada, "Cognitive maritime wireless mesh/ad hoc networks," *J. Netw. Comput. Appl.*, vol. 35, no. 2, pp. 518–526, Mar. 2012.

[6] *Maritime Broadband Wireless Mech Networks*, document ITU-R M. 2202, Nov. 2010.

[7] M. J. Lopes, F. Teixeira, J. B. Mamede, and R. Campos, "Wi-Fi broadband maritime communications using 5.8 GHz band," in *Proc. Underwater Commun. Netw. (UComms)*, Sestri Levante, Italy, Sep. 2014, pp. 1–5.

[8] L. Santos, "Wi-Fi maritime communications using TV white spaces," M.S. thesis, Fac. Eng., Univ. Porto, Porto, Portugal, Jul. 2013.

[9] L. Bastos and H. Wietgrefe, "WiMAX for highly deployable mission-critical communications networks," in *Proc. IEEE Mil. Commun. Conf. (MILCOM)*, Orlando, FL, USA, Oct. 2007, pp. 1–7.

[10] R. G. Garroppo, S. Giordano, and D. Iacono, "Experimental and simulation study of a WiMAX system in the sea port scenario," in *Proc. IEEE Int. Conf. Commun. (ICC)*, Dresden, Germany, Jun. 2009, pp. 1–5.

[11] R. G. Garroppo, S. Giordano, D. Iacono, A. Cignoni, and M. Falzarano, "WiMAX testbed for interconnection of mobile navy units in operational scenarios," in *Proc. IEEE Mil. Commun. Conf. (MILCOM)*, San Diego, CA, USA, Nov. 2008, pp. 1–7.

[12] M. S. Choi, S. Park, Y. Lee, and S. R. Lee, "Ship to ship maritime communication for e-Navigation using WiMAX," *Int. J. Multimedia Ubiquitous Eng.*, vol. 9, no. 4, pp. 171–178, Apr. 2014.

[13] P.-Y. Kong *et al.*, "A performance comparison of routing protocols for maritime wireless mesh networks," in *Proc. IEEE Wireless Commun. Netw. Conf.*, Las Vegas, NV, USA, Mar./Apr. 2008, pp. 2170–2175.

[14] Y. Xu, S. Jiang, and F. Liu, "A LTE-based communication architecture for coastal networks," in *Proc. 11th ACM Int. Conf. Underwater Netw. Syst. (WUWNet)*, New York, NY, USA, 2016, pp. 6:1–6:2.

[15] F. Arreghini, R. Agrone, P. Danielli, and A. Pigni, "Heterogeneous network testbed for tactical communication in shore scenario," in *Proc. Mil. Commun. Conf. (MILCOM)*, Oct. 2015, pp. 483–488.

[16] S. M. Anwar, E. Goron, Y. Toutain, J. P. Péronne, and S. Héthuin, "LTE terminal for maritime applications," in *Proc. Mil. Commun. Inf. Syst. Conf. (MCC)*, St.-Malo, France, Oct. 2013, pp. 1–4.

[17] M.-T. Zhou *et al.*, "TRITON: High-speed maritime wireless mesh network," *IEEE Wireless Commun.*, vol. 20, no. 5, pp. 134–142, Oct. 2013.

[18] Y. Kim, J. Kim, Y. Wang, K. Chang, J. W. Park, and Y. Lim, "Application scenarios of nautical Ad-Hoc network for maritime communications," in *Proc. OCEANS*, Biloxi, MS, USA, Oct. 2009, pp. 1–4.

[19] F. Bekkada and K. Yang, "Novel maritime communications technologies," in *Proc. Medit. Microw. Symp. (MMS)*, Aug. 2010, pp. 338–341.

[20] R. Campos, T. Oliveira, N. Cruz, A. Matos, and J. M. Almeida, "BLUECOM+: Cost-effective broadband communications at remote ocean areas," in *Proc. OCEANS*, Shanghai, China, Apr. 2016, pp. 1–6.

[21] F. B. Teixeira *et al.*, "Enabling broadband Internet access offshore using tethered balloons: The BLUECOM+ experience," in *Proc. OCEANS*, Aberdeen, U.K., Jun. 2017, pp. 1–7.

[22] J. Braga, F. Balampanis, A. P. Aguiar, J. Sousa, I. Maza, and A. Ollero, "Coordinated efficient buoys data collection in large complex coastal environments using UAVs," in *Proc. OCEANS*, Anchorage, AK, USA, Sep. 2017, pp. 1–9.

[23] T. Yang, Z. Cui, R. Wang, J. Zhao, Z. Su, and R. Deng, "A multi-vessels cooperation scheduling for networked maritime fog-ran architecture leveraging SDN," *Peer-to-Peer Netw. Appl.*, vol. 11, no. 4, pp. 808–820, Jul. 2018.

[24] Y. Xu, "Quality of service provisions for maritime communications based on cellular networks," *IEEE Access*, vol. 5, pp. 23881–23890, 2017.

[25] *LTE, Wifi and 5G Massive MIMO Communications in Maritime Propagation Environment (MAMIME)*, Research Council of Norway, Oslo, Norway, Apr. 2019.

[26] J. Hagenauer, F. Dolainsky, E. Lutz, W. Papke, and R. Schweikert, "The maritime satellite communication channel–channel model, performance of modulation and coding," *IEEE J. Sel. Areas Commun.*, vol. JSAC-5, no. 4, pp. 701–713, May 1987.

[27] J.-H. Lee, J. Choi, W.-H. Lee, J.-W. Choi, and S.-C. Kim, "Measurement and analysis on land-to-ship offshore wireless channel in 2.4 GHz," *IEEE Wireless Commun. Lett.*, vol. 6, no. 2, pp. 222–225, Apr. 2017.

[28] K. Yang, T. Røste, F. Bekkadal, and T. Ekman, "Channel characterization including path loss and Doppler effects with sea reflections for mobile radio propagation over sea at 2 GHz," in *Proc. Int. Conf. Wireless Commun. Signal Process. (WCSP)*, Suzhou, China, Oct. 2010, pp. 1–6.

[29] W. Wang, R. Raulefs, and T. Jost, "Fading characteristics of ship-to-land propagation channel at 5.2 GHz," in *Proc. OCEANS*, Shanghai, China, Apr. 2016, pp. 1–7.

[30] Y. H. Lee, F. Dong, and Y. S. Meng, "Near sea-surface mobile radiowave propagation at 5 GHz: Measurements and modeling," *Radioengineering*, vol. 23, no. 3, pp. 824–830, 2014.

[31] W. Wang, G. Hoerack, T. Jost, R. Raulefs, M. Walter, and U. C. Fiebig, "Propagation channel at 5.2 GHz in baltic sea with focus on scattering phenomena," in *Proc. 9th Eur. Conf. Antennas Propag. (EuCAP)*, Lisbon, Portugal, Apr. 2015, pp. 1–5.

[32] W. Wang, T. Jost, and R. Raulefs, "Large scale characteristics of ship-to-land propagation at 5.2 GHz in harbor environment," in *Proc. IEEE 82nd Veh. Tech. Conf. (VTC-Fall)*, Boston, MA, USA, Sep. 2015, pp. 1–5.

[33] J. C. Reyes-Guerrero, M. Bruno, L. A. Mariscal, and A. Medouri, "Buoy-to-ship experimental measurements over sea at 5.8 GHz near urban environments," in *Proc. 11th Medit. Microw. Symp. (MMS)*, Hammamet, Tunisia, Sep. 2011, pp. 320–324.

[34] J. C. Reyes-Guerrero and L. A. Mariscal, "5.8 GHz propagation of low-height wireless links in sea port scenario," *Electron. Lett.*, vol. 50, no. 9, pp. 710–712, Apr. 2014.

[35] N. Mehrnia and M. K. Ozdemir, "Novel maritime channel models for millimeter radiowaves," in *Proc. 24th Int. Conf. Softw., Telecommun. Comput. Netw. (SoftCOM)*, Split, Croatia, Sep. 2016, pp. 1–6.

[36] Q. Lei and M. Rice, "Multipath channel model for over-water aeronautical telemetry," *IEEE Trans. Aerosp. Electron. Syst.*, vol. 45, no. 2, pp. 735–742, Apr. 2009.

[37] Y. S. Meng and Y. H. Lee, "Measurements and characterizations of air-to-ground channel over sea surface at C-band with low airborne altitudes," *IEEE Trans. Veh. Technol.*, vol. 60, no. 4, pp. 1943–1948, May 2011.

[38] D. W. Matolak and R. Sun, "Air–ground channel characterization for unmanned aircraft systems—Part I: Methods, measurements, and models for over-water settings," *IEEE Trans. Veh. Technol.*, vol. 66, no. 1, pp. 26–44, Jan. 2017.

[39] H. Mo, B. Chen, and C. Shen, "Radio propagation prediction model for maritime mobile communication," in *Proc. IET Int. Conf. Wireless Commun. Appl. (ICWCA)*, Kuala Lumpur, Malaysia, 2012, pp. 1–5.

[40] Y. Zhao, J. Ren, and X. Chi, "Maritime mobile channel transmission model based on ITM," in *Proc. 2nd Int. Symp. Comput., Commun., Control Autom.*, 2013, pp. 378–383.

[41] *ITU-R Recommendation P.1546-5: Method for Point-to-Area Predictions for Terrestrial Services in the Frequency Range 30 MHz to 3000 MHz*, ITU, Geneva, Switzerland, Sep. 2013.

[42] H. Wang, W. Du, and X. Chen, "Evaluation of radio over sea propagation based ITU-R recommendation P.1546-5," *J. Commun.*, vol. 10, no. 4, pp. 231–237, Apr. 2015.

[43] J. Joe *et al.*, "Path loss measurements in sea port for WiMAX," in *Proc. Wireless Commun. Netw. Conf.*, Kowloon, China, Jun. 2007, pp. 1871–1876.

[44] Y. M. Le Roux, J. Ménard, C. Toquin, J.-P. Jolivet, and F. Nicolas, "Experimental measurements of propagation characteristics for maritime radio links," in *Proc. 9th Int. Conf. Intell. Transport Syst. Telecommun. (ITST)*, Lille, France, Oct. 2009, pp. 364–369.

[45] A. V. Castro *et al.*, "Experimental assessment of propagation models over sea for UHF and X bands," in *Proc. IEEE Int. Symp. Antennas Propag. (APSURSI)*, Fajardo, Puerto Rico, Jun./Jul. 2016, pp. 2059–2060.

[46] Y. H. Lee and Y. S. Meng, "Key considerations in the modeling of tropical maritime microwave attenuations," *Int. J. Antennas Propag.*, vol. 2015, 2015, Art. no. 246793, doi: 10.1155/2015/246793.

[47] F. Huang, X. Liao, and Y. Bai, "Multipath channel model for radio propagation over sea surface," *Wireless Pers. Commun.*, vol. 90, no. 1, pp. 245–257, 2016.

[48] X. Su, H. Yu, K. Chang, S.-G. Kim, and Y.-K. Lim, "Case study for ship Ad-hoc networks under a maritime channel model in coastline areas," *KSII Trans. Internet Inf. Syst.*, vol. 9, no. 10, pp. 4002–4014, Oct. 2015.

[49] H. Wang and W. Du, "Research on maritime radio wave multipath propagation based on stochastic ray method," *Math. Problems Eng.*, vol. 2016, 2016, Art. no. 5178136, doi: 10.1155/2016/5178136.

[50] X. Cao and T. Jiang, "Research on sea surface Ka-band stochastic multipath channel modeling," in *Proc. 3rd Asia–Pacific Conf. Antennas Propag.*, Harbin, China, Jul. 2014, pp. 675–678.

[51] X. Zhao and P. Yang, "A simple two-dimensional ray-tracing visual tool in the complex tropospheric environment," *Atmosphere*, vol. 8, no. 2, p. 35, Feb. 2017.

[52] E. Dinc and O. B. Akan, "Channel model for the surface ducts: Large-scale path-loss, delay spread, and AOA," *IEEE Trans. Antennas Propag.*, vol. 63, no. 6, pp. 2728–2738, Jun. 2015.

[53] E. Dinc and O. B. Akan, "Beyond-line-of-sight communications with ducting layer," *IEEE Commun. Mag.*, vol. 52, no. 10, pp. 37–43, Oct. 2014.

[54] E. Dinc and O. B. Akan, "Beyond-line-of-sight ducting channels: Coherence bandwidth, coherence time and rain attenuation," *IEEE Commun. Lett.*, vol. 19, no. 12, pp. 2274–2277, Dec. 2015.

[55] E. Dinc, F. Alagoz, and O. B. Akan, "Path-Loss and correlation analysis for space and polarization diversity in surface ducts," *IEEE Trans. Antennas Propag.*, vol. 64, no. 10, pp. 4498–4503, Oct. 2016.

[56] X.-L. Zhao, J.-Y. Huang, and S.-H. Gong, "Statistical analysis of an over-the-sea experimental transhorizon communication at X-band in China," *J. Electromagn. Waves Appl.*, vol. 22, no. 10, pp. 1430–1439, 2008.

[57] K. S. Zaidi, V. Jeoti, A. Iqbal, and A. Awang, "Feasibility of trans-horizon, high-capacity maritime wireless backhaul communication link," in *Proc. 5th Int. Conf. Intell. Adv. Syst. (ICIAS)*, Kuala Lumpur, Malaysia, Jun. 2014, pp. 1–6.

[58] H. V. Hitney and L. R. Hitney, "Frequency diversity effects of evaporation duct propagation," *IEEE Trans. Antennas Propag.*, vol. 38, no. 10, pp. 1694–1700, Oct. 1990.

[59] I. J. M. Heemskerk and R. B. Boekema, "The influence of evaporation duct on the propagation of electromagnetic waves low above the sea surface at 3-94 GHz," in *Proc. 8th Int. Conf. Antennas Propag.*, Edinburgh, U.K., Mar./Apr. 1993, pp. 348–351.

[60] C. Palazzi, G. Woods, I. Atkinson, and S. Kininmonth, "High speed over ocean radio link to great barrier reef," in *Proc. IEEE Region 10 Conf. (TENCON)*, Melbourne, QLD, Australia, Nov. 2005, pp. 1–6.

[61] G. S. Woods, A. Ruxton, C. Huddlestone-Holmes, and G. Gigan, "High-capacity, long-range, over ocean microwave link using the evaporation duct," *IEEE J. Ocean. Eng.*, vol. 34, no. 3, pp. 323–330, Jul. 2009.

[62] Y. H. Lee and Y. S. Meng, "Empirical modeling of ducting effects on a mobile microwave link over a sea surface," *Radioengineering*, vol. 21, no. 4, pp. 1054–1059, 2012.

[63] K. S. Zaidi, V. Jeoti, A. Awang, and M. Drieberg, "High reliability using virtual MIMO based mesh network for maritime wireless communication," in *Proc. 6th Int. Conf. Intell. Adv. Syst. (ICIAS)*, Kuala Lumpur, Malaysia, Aug. 2016, pp. 1–5.

[64] W. U. Bajwa, A. Sayeed, and R. Nowak, "Sparse multipath channels: Modeling and estimation," in *Proc. IEEE 13th Digit. Signal Process. Workshop, 5th IEEE Signal Process. Educ. Workshop*, Marco Island, FL, USA, Jan. 2009, pp. 320–325.

[65] A. A. M. Saleh and R. A. Valenzuela, "A statistical model for indoor multipath propagation," *IEEE J. Sel. Areas Commun.*, vol. 5, no. 2, pp. 128–137, Feb. 1987.

[66] G. D. Durgin, T. S. Rappaport, and D. A. de Wolf, "New analytical models and probability density functions for fading in wireless communications," *IEEE Trans. Commun.*, vol. 50, no. 6, pp. 1005–1015, Jun. 2002.

[67] J. M. Romero-Jerez, F. J. Lopez-Martinez, J. F. Paris, and A. Goldsmith, "The fluctuating two-ray fading model for mmWave communications," in *Proc. IEEE Globecom Workshops (GC Wkshps)*, Washington, DC, USA, Dec. 2016, pp. 1–6.

[68] J. M. Romero-Jerez, F. J. Lopez-Martinez, J. F. Paris, and A. J. Goldsmith, "The fluctuating two-ray fading model: Statistical characterization and performance analysis," *IEEE Trans. Commun.*, vol. 16, no. 7, pp. 4420–4432, Jul. 2017.

[69] W. L. Stutzman and W. K. Dishman, "A simple model for the estimation of rain-induced attenuation along earth-space paths at millimeter wavelengths," *Radio Sci.*, vol. 17, no. 6, pp. 1465–1476, Nov./Dec. 1982.

[70] C. Amaya and D. V. Rogers, "Characteristics of rain fading on Ka-band satellite-earth links in a Pacific maritime climate," *IEEE Trans. Microw. Theory Techn.*, vol. 50, no. 1, pp. 41–45, Jan. 2002.

[71] T. Keshav, S. Yoon, and S. R. Lee, "Compensating the effect of ship rocking in maritime ship-to-shore communication," *J. Korean Inst. Commun. Inf. Sci.*, vol. 38C, no. 3, pp. 271–277, 2013.

[72] Y. Zhao, M. Zhang, H. Chen, and X.-F. Yuan, "Radar scattering from the composite ship-ocean scene: Doppler spectrum analysis based on the motion of six degrees of freedom," *IEEE Trans. Antennas Propag.*, vol. 62, no. 8, pp. 4341–4347, Aug. 2014.

[73] D. Reddy, V. Parthasarathy, and S. N. Rao, "Analysis of the effect of waves on the stability of TDMA based marine long range Wi-Fi backhaul links," in *Proc. IEEE Int. Conf. Comput. Intelligence Comput. Res. (ICCIC)*, Chennai, India, Dec. 2016, pp. 1–8.

[74] C.-W. Ang and S. Wen, "Signal strength sensitivity and its effects on routing in maritime wireless networks," in *Proc. 33rd IEEE Conf. Local Comput. Netw. (LCN)*, Montreal, QUE, Canada, Oct. 2008, pp. 192–199.

[75] W. Hubert, Y.-M. Le Roux, M. Ney, and A. Flamand, "Impact of ship motions on maritime radio links," *Int. J. Antennas Propag.*, vol. 2012, 2012, Art. no. 507094, doi: 10.1155/2012/507094.

[76] F. Huang, Y. Bai, and W. Du, "Maritime radio propagation with the effects of ship motions," *J. Commun.*, vol. 10, no. 5, pp. 345–351, May 2015.

[77] W. J. Pierson, Jr. and L. Moskowitz, "A proposed spectral form for fully developed wind seas based on the similarity theory of S. A. Kitaigorodskii," *J. Geophys. Res.*, vol. 69, no. 24, pp. 5181–5190, Dec. 1964.

[78] Y. Karasawa and T. Shiokawa, "Characteristics of L-band multipath fading due to sea surface reflection," *IEEE Trans. Antennas Propag.*, vol. AP-32, no. 6, pp. 618–623, Jun. 1984.

[79] R. A. Paulus, "Evaporation duct effects on sea clutter," *IEEE Trans. Antennas Propag.*, vol. 38, no. 11, pp. 1765–1771, Nov. 1990.

[80] K. Yang, Q. Zhang, Y. Shi, Z. He, B. Lei, and Y. Han, "On analyzing space-time distribution of evaporation duct height over the global ocean," *Acta Oceanologica Sin.*, vol. 35, no. 7, pp. 20–29, Aug. 2016.

[81] A. K. Widiawan and R. Tafazolli, "High altitude platform station (HAPS): A review of new infrastructure development for future wireless communications," *Wireless Pers. Commun.*, vol. 42, no. 3, pp. 387–404, Aug. 2007.

[82] D. W. Matolak and R. Sun, "Unmanned aircraft systems: Air-ground channel characterization for future applications," *IEEE Veh. Technol. Mag.*, vol. 10, no. 2, pp. 79–85, Jun. 2015.

[83] W. Wang, R. Raulefs, and T. Jost, "Fading characteristics of maritime propagation channel for beyond geometrical horizon communications in C-band," *CECS Space J.*, pp. 1–10, Dec. 2017, doi: 10.1007/s12567-017-0185-1.

[84] S. Jeon, Z. Yim, and J.-S. Seo, "Path loss model for coupling loop interference with multiple reflections over single frequency network," *IETE Tech. Rev.*, vol. 29, no. 6, pp. 499–505, 2012.

[85] A. G. Longley and P. L. Rice, "Prediction of tropospheric radio transmission loss over irregular terrain," U.S. Dept. Commerce, Inst. Telecommun. Sci., Boulder, CO, USA, ESSA Tech. Rep. ERL 79-ITS, vol. 67, Jul. 1968.

[86] "Electromagnetic compatibility and radio spectrum matters (ERM); System reference document (SRdoc); Broadband communication links for ships and fixed installations engaged in off-shore activities operating in the 5 GHz to 8 Ghz range," ETSI, Sophia Antipolis, France, Tech. Rep. 103 109 v1.1.1, Nov. 2013.

[87] X. Yin and X. Cheng, "Geometry-based stochastic channel modeling," in *Propagation Channel Characterization, Parameter Estimation, and Modeling for Wireless Communications*. Singapore: Wiley, Sep. 2016, pp. 77–105.

[88] I. Sirkova, "Brief review on pe method application to propagation channel modeling in sea environment," *Open Eng.*, vol. 2, no. 1, pp. 19–38, Mar. 2012.

[89] R. Akbarpour and A. R. Webster, "Ray-tracing and parabolic equation methods in the modeling of a tropospheric microwave link," *IEEE Trans. Antennas Propag.*, vol. 53, no. 11, pp. 3785–3791, Nov. 2005.

[90] P. Zhang, L. Bai, Z. Wu, and L. Guo, "Applying the parabolic equation to tropospheric groundwave propagation: A review of recent achievements and significant milestones," *IEEE Antennas Propag. Mag.*, vol. 58, no. 3, pp. 31–44, Jun. 2016.

[91] N. E. Lentini and E. E. Hackett, "Global sensitivity of parabolic equation radar wave propagation simulation to sea state and atmospheric refractivity structure," *Radio Sci.*, vol. 50, no. 10, pp. 1027–1049, Oct. 2015.

[92] Z. Yun and M. F. Iskander, "Ray tracing for radio propagation modeling: Principles and applications," *IEEE Access*, vol. 3, pp. 1089–1100, 2015.

[93] H. Zhou, J. Wang, Q. Sun, W. Feng, L. You, and C. Xu, "A ray-optics approach for evaporation duct channel modeling," in *Proc. IEEE Wireless Commun. Signal Process. Conf. (WCSP)*, Hangzhou, China, Oct. 2018, pp. 1–6.

[94] A. E. Barrios, K. Anderson, and G. Lindem, "Low altitude propagation effects—A validation study of the advanced propagation model (APM) for mobile radio applications," *IEEE Trans. Antennas. Propag.*, vol. 54, no. 10, pp. 2869–2877, Oct. 2006.

[95] A. Coker, L. Straatemeier, T. Rogers, P. Valdez, D. Cooksey, and K. Griendling, "Maritime channel modeling and simulation for efficient wideband communications between autonomous unmanned surface vehicles," in *Proc. OCEANS*, San Diego, CA, USA, Sep. 2013, pp. 1–9.

[96] E. Dinc and O. B. Akan, "Correction to 'channel model for the surface ducts: Large-scale path-loss, delay spread, and AOA,'" *IEEE Trans. Antennas. Propag.*, vol. 64, no. 8, pp. 3735–3736, Aug. 2016.

[97] K. S. Zaidi, V. Jeoti, M. Drieberg, A. Awang, and A. Iqbal, "Long-range mobile communication over sea utilizing evaporation duct," in *Proc. Progr. Electromagn. Res. Symp. Fall (PIERS-FALL)*, Singapore, Nov. 2017, pp. 846–850.

[98] A. S. Kulessa *et al.*, "The tropical air–sea propagation study (TAPS)," *Bull. Amer. Meteorol. Soc.*, vol. 98, no. 3, pp. 517–537, Mar. 2017.

[99] L. Sevgi, "A ray-shooting visualization Matlab package for 2D groundwave propagation simulations," *IEEE Antennas. Propag. Mag.*, vol. 46, no. 4, pp. 140–145, Apr. 2004.

[100] K. R. Schaubach, N. J. Davis, and T. S. Rappaport, "A ray tracing method for predicting path loss and delay spread in microcellular environments," in *Proc. IEEE Veh. Technol. Conf. (VTC)*, May 1992, pp. 932–935.

[101] X. Shen, J. Austin, and E. Vilar, "Modelling enhanced spherical diffraction and troposcattering on a transhorizon path with the aid of the parabolic equation and ray tracing methods," in *Proc. IEE Colloq. Common Model. Techn. Electromagn. Wave Acoustic Wave Propag.*, London, U.K., Mar. 1996, pp. 1–7.

[102] O. El Ayach, S. Rajagopal, S. Abu-Surra, Z. Pi, and R. W. Heath, Jr., "Spatially sparse precoding in millimeter wave MIMO systems," *IEEE Trans. Wireless Commun.*, vol. 13, no. 3, pp. 1499–1513, Mar. 2014.

[103] Q. Zhang, K. Yang, Y. Shi, and X. Yan, "Oceanic propagation measurement in the northern part of the south China sea," in *Proc. OCEANS*, Shanghai, China, Apr. 2016, pp. 1–4.

[104] W. Wang, R. Raulefs, T. Jost, A. Dammann, C. Gentner, and S. Zhang, "Ship-to-land broadband channel measurement campaign at 5.2 GHz," in *Proc. Oceans*, St. John's, NL, Canada, Sep. 2014, pp. 1–8.

[105] J. C. Reyes-Guerrero, "Experimental broadband channel characterization in a sea port environment at 5.8 GHz," *IEEE J. Ocean. Eng.*, vol. 41, no. 3, pp. 509–514, Jul. 2016.

[106] W. Wang, T. Jost, and R. Raulefs, "A semi-deterministic path loss model for in-harbor LoS and NLoS environment," *IEEE Trans. Antennas. Propag.*, vol. 65, no. 12, pp. 7399–7404, Dec. 2017.

[107] J. Wang, S. Jin, X. Gao, K.-K. Wong, and E. Au, "Statistical Eigenmode-based SDMA for two-user downlink," *IEEE Trans. Signal Process.*, vol. 60, no. 10, pp. 5371–5383, Oct. 2012.

[108] J. Wang, M. Matthaiou, S. Jin, and X. Gao, "Precoder design for multiuser MISO systems exploiting statistical and outdated CSIT," *IEEE Trans. Commun.*, vol. 61, no. 11, pp. 4551–4564, Nov. 2013.

[109] C. Liu, W. Feng, T. We, and N. Ge, "Fairness-oriented hybrid precoding for massive MIMO maritime downlink systems with large-scale CSIT," *China Commun.*, vol. 15, no. 1, pp. 52–61, Jan. 2018.

[110] E. Dinc and O. B. Akan, "Limited feedback multi-stage beam-forming method for beyond-line-of-sight ducting channels," in *Proc. Mil. Commun. Conf. (MILCOM)*, Tampa, FL, USA, Oct. 2015, pp. 547–552.

[111] Y. Li, J. Wang, S. Zhang, Z. Bao, and J. Wang, "Efficient coastal communications with sparse network coding," *IEEE Netw. Mag.*, vol. 32, no. 4, pp. 122–128, Jul./Aug. 2018.

[112] C.-X. Wang, S. Wu, L. Bai, X. You, J. Wang, and C.-L. I, "Recent advances and future challenges for massive MIMO channel measurements and models," *Sci. China Inf. Sci.*, vol. 59, no. 2, p. 021301, Feb. 2016.

[113] L. Liu, D. W. Matolak, C. Tao, Y. Lu, and H. Chen, "Far region boundary definition of linear massive MIMO antenna arrays," in *Proc. IEEE 82nd Veh. Technol. Conf. (VTC Fall)*, Sep. 2015, pp. 1–6.

[114] A. Danklmayer, G. Biegel, T. Brehm, S. Sieger, and J. Förster, "Millimeter wave propagation above the sea surface during the squirrel campaign," in *Proc. 16th Int. Radar Symp.*, Dresden, Germany, Jun. 2015, pp. 300–304.

[115] A. Dankmlayer, P. Colditz, G. Biegel, T. Brehm, and J. Förster, "North sea millimeterwave propagation experiment: The Sylt campaign," in *Proc. 17th Int. Radar Symp.*, Krakow, Poland, May 2016, pp. 1–5.

[116] A. Danklmayer, T. Brehm, G. Biegel, and J. Förster, "Multi-frequency propagation measurements over a horizontal path above the sea surface in the Baltic Sea," in *Proc. 7th Eur. Conf. Antennas Propag. (EuCAP)*, Gothenburg, Sweden, Apr. 2013, pp. 2526–2527.

[117] H. Ye, G. Y. Li, B.-H. F. Juang, and K. Sivanesan. (Jul. 2018). "Channel agnostic end-to-end learning based communication systems with conditional GAN." [Online]. Available: https://arxiv.org/abs/1807.00447

JUE WANG (S'10–M'14) received the B.S. degree in communications engineering from Nanjing University, Nanjing, China, in 2006, and the M.S. and Ph.D. degrees from the National Communications Research Laboratory, Southeast University, Nanjing, China, in 2009 and 2014, respectively. From 2014 to 2016, he was with the Singapore University of Technology and Design as a Post-Doctoral Research Fellow. He is currently with the School of Electronic and Information Engineering, Nantong University, Nantong, China.

His research interests include MIMO wireless communications, multiuser transmission, MIMO channel modeling, massive MIMO systems, and physical layer security. He has served as a Technical Program Committee Member for a number of IEEE conferences, and reviewer for various IEEE journals. He was awarded as an Exemplary Reviewer of the IEEE TRANSACTIONS ON COMMUNICATIONS in 2014.

HAIFENG ZHOU received the B.S. degree from Nantong University, China, in 2016, where he is currently pursuing the M.S. degree with the School of Electronics Information. His research interests include wireless channel modeling and machine learning.

YE LI (M'17) received the B.S. and M.S. degrees in electrical engineering from Southeast University, Nanjing, China, in 2007 and 2010, respectively, and the Ph.D. degree from Queen's University, Kingston, ON, Canada, in 2014. From 2014 to 2016, he was with IBM Canada Ltd., Markham, ON, Canada. He has been a Lecturer with the School of Electronics and Information, Nantong University, Nantong, China, since 2016. His main research interests are in network coding and wireless communication networks.

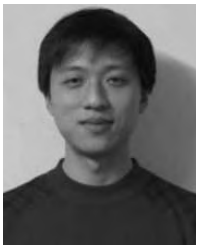

QIANG SUN received the Ph.D. degree in communications and information systems from Southeast University, Nanjing, in 2014. He was a Visiting Scholar with the University of Delaware, USA, in 2016. He is currently an Associate Professor with the School of Electronics and Information, Nantong University, Nantong, China. His research interests include deep learning and wireless communications.

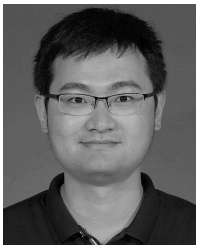

YONGPENG WU (S'08–M'13–SM'17) received the B.S. degree in telecommunication engineering from Wuhan University, Wuhan, China, in 2007, and the Ph.D. degree in communication and signal processing with the National Mobile Communications Research Laboratory, Southeast University, Nanjing, China, in 2013.

He was a Senior Research Fellow with the Institute for Communications Engineering, Technical University of Munich, Germany, and the Humboldt Research Fellow and the Senior Research Fellow with the Institute for Digital Communications, University Erlangen-Nürnberg, Germany. During his Ph.D. studies, he conducted cooperative research at the Department of Electrical Engineering, Missouri University of Science and Technology, USA. He is currently a Tenure-Track Associate Professor with the Department of Electronic Engineering, Shanghai Jiao Tong University, China. His research interests include massive MIMO/MIMO systems, physical layer security, signal processing for wireless communications, and multivariate statistical theory.

Dr. Wu has been a TPC member of various conferences, including GLOBECOM, ICC, VTC, and PIMRC. He received the IEEE Student Travel Grants for the IEEE International Conference on Communications (ICC) in 2010, the Alexander von Humboldt Fellowship in 2014, the Travel Grants for IEEE Communication Theory Workshop in 2016, the Excellent Doctoral Thesis Awards of China Communications Society in 2016, the Exemplary Editor Award of the IEEE Communication Letters 2017, and the Young Elite Scientist Sponsorship Program by CAST 2017. He is currently an Editor of the IEEE Access and the IEEE Communications Letters. He was the lead guest editor for the special issue Physical Layer Security for 5G Wireless Networks of the IEEE Journal on Selected Areas in Communications. He was an Exemplary Reviewer of the IEEE Transactions on Communications in 2015 and 2016.

SHI JIN received the Ph.D. degree in information and communications engineering from Southeast University, Nanjing, in 2007. From 2007 to 2009, he was a Research Fellow with the Adastral Park Research Campus, University College London, London, U.K. He is currently with the Faculty of the National Mobile Communications Research Laboratory, Southeast University. His research interests include space time wireless communications, random matrix theory, and information theory. He and his co-authors received the 2011 IEEE Communications Society Stephen O. Rice Prize Paper Award in the field of communication theory and the 2010 Young Author Best Paper Award by the IEEE Signal Processing Society. He serves as an Associate Editor of the IEEE Transactions on Wireless Communications, the IEEE Communications Letters, and *IET Communications*.

TONY Q. S. QUEK (S'98–M'08–SM'12–F'18) received the B.E. and M.E. degrees in electrical and electronics engineering from the Tokyo Institute of Technology and the Ph.D. degree in electrical engineering and computer science from MIT. He is currently a tenured Associate Professor with the Singapore University of Technology and Design (SUTD). He also serves as the Associate Head of ISTD Pillar and the Deputy Director of the SUTD-ZJU IDEA. His main research interests are the application of mathematical, optimization, and statistical theories to wireless communication, networking, signal processing, and resource allocation problems. Specific current research topics include network intelligence, wireless security, Internet-of-Things, and big data processing.

He has co-authored the book *Small Cell Networks: Deployment, PHY Techniques, and Resource Allocation* (Cambridge University Press, 2013) and the book *Cloud Radio Access Networks: Principles, Technologies, and Applications* (Cambridge University Press, 2017). He has been actively involved in organizing and chairing sessions, and has served as a member of the technical program committee and a symposium chair in a number of international conferences. He is currently an elected member of the IEEE Signal Processing Society SPCOM Technical Committee. He was an Executive Editorial Committee Member for the IEEE Transactions on Wireless Communications, an Editor for the IEEE Transactions on Communications, and an Editor for the IEEE Wireless Communications Letters.

Dr. Quek was honored with the 2008 Philip Yeo Prize for Outstanding Achievement in Research, the IEEE GLOBECOM 2010 Best Paper Award, the 2012 IEEE William R. Bennett Prize, the IEEE SPAWC 2013 Best Student Paper Award, the IEEE WCSP 2014 Best Paper Award, the 2015 SUTD Outstanding Education Awards Excellence in Research, the 2016 Thomson Reuters Highly Cited Researcher, the 2016 IEEE Signal Processing Society Young Author Best Paper Award, and the 2017 IEEE Communications Society Asia Pacific Outstanding Paper Award.

CHEN XU was born in Nantong, China. He was with Dean of the Key Laboratory of ASIC Design of Jiangsu Province, Jiangsu, China. He is currently a Professor with the School of Electronics and Information, Nantong University, Nantong, China. His research interests include machine learning, image processing, intelligent transportation system, medical information processing, and wireless communications.